

Influence of vesicular glutamate leakage on synaptic transmission at the mammalian presynaptic terminal

DOCTORAL DISSERTATION

A thesis submitted in partial fulfillment of the requirements for the degree of Doctor of Philosophy

By:

Chihiro Takami

Supervisor:

Dr. Shigeo Takamori

Graduated School of Brain Science

Doshisha University

March 2017

Kyoto, Japan

Table of contents

Abstract	1
----------------	---

List of Figures	3
-----------------------	---

1. Introduction

1.1. Synaptic transmission	4
1.2. Parameters that determine the strength of neurotransmission	7
1.3. Synaptic vesicle recycling.....	10
1.3.1. Exocytosis	10
1.3.2. Endocytosis	11
1.3.3. Re-acidification.....	12
1.3.4. Vesicular neurotransmitter uptake.....	14
1.4. Functional vesicle pools.....	17
1.5. Presynaptic regulation of quantal size	19
1.5.1. Cytosolic neurotransmitter concentrations.....	20
1.5.2. Regulation of the driving force	21
1.5.3. Transporter expression	22
1.5.4. Leakage at equilibrium.....	23
1.6. Aim of this work	25
1.7. Calyx of Held.....	26

2. Materials and Methods

2.1. Ethical approval	28
2.2. Preparation of slices for patch clamp experiments	28
2.2.1. Slicing	28
2.2.2. Mechanical fixation for recording	29
2.2.3. Optical setup	30
2.3. Whole-cell patch clamp recordings	30
2.3.1. Whole-cell recording	30
2.3.2. Simultaneous pre- and postsynaptic recordings	31
2.4. Capacitance measurement	33

2.5. Variance-mean analysis	34
2.6. Analysis of electrophysiological data	36
2.6.1. Detection of mEPSCs with a scaled template	36
2.6.2. mEPSC amplitude compensation	37
2.7. Statistical analysis	38
3. Results	
3.1. Washout of presynaptic cytosolic glutamate	39
3.2. Block of vacuolar ATPase with bafilomycin A1	41
3.3. mEPSCs reduced by CNQX	43
3.4. Influence of filling state on vesicle recycling	46
3.5. Quantal size can be monitored during high frequency stimulation by the non-stationary variance-mean analysis.	48
3.6. The variance-mean analysis reliably reports changes of quantal size during repetitive stimulation.....	53
3.7. Quantal size during repetitive stimulation markedly decreased in the absence of cytosolic glutamate.....	55
4. Discussion	60
Appendix. Technical concerns on the non-stationary fluctuation analysis	64
Acknowledgments.....	66
Bibliography.....	68

Abstract

Since the amount of neurotransmitters in single synaptic vesicles ultimately defines the strength of neurotransmission, it is important to understand how neurotransmitters are concentrated and maintained in synaptic vesicles at the presynaptic terminals. Although previous studies have suggested that both the neurotransmitter uptake and leakage can regulate the amount of neurotransmitter content, relative contribution of neurotransmitter leakage from synaptic vesicles to synaptic transmission has caught little attention. While the major excitatory neurotransmitter glutamate leaks out of synaptic vesicles relatively fast when trans-vesicular proton gradient is dissipated in isolated vesicle preparations, it is controversial whether glutamate can also leak out of vesicles in the nerve terminal. To address this issue, I abolished vesicular glutamate uptake by washing out presynaptic cytosolic glutamate in whole-cell dialysis, or by blocking vacuolar-type H⁺ ATPase using bafilomycin A₁ (Baf) at the calyx of Held synapses in mice brainstem slices. Then, I postsynaptically recorded the miniature excitatory postsynaptic currents (mEPSCs), each of which is elicited by neurotransmitters released from a single vesicle, thereby a good readout of the vesicular neurotransmitter content.

Both presynaptic glutamate washout and Baf application reduced the mean amplitude and frequency of mEPSCs and the mean amplitude of EPSCs evoked every 10 min, which are evoked by neurotransmitters released from multiple vesicles. However, the percentage reduction of mEPSC amplitude was much less than those of EPSC amplitude and mEPSC frequency, and tended to reach a plateau. One possible reason is that the postsynaptic receptors failed to detect small amount of

glutamate released from partially-filled vesicles. The amplitude of mEPSCs after glutamate washout or Baf application sustained high above the detection limit which was deduced from the reduction of mEPSC amplitude by an AMPA receptor blocker, CNQX. In addition, membrane capacitance measurements from the presynaptic terminals indicated no effect of glutamate washout on exocytosis or endocytosis of synaptic vesicles, indicating that the amount of glutamate in the lumen did not affect synaptic vesicle recycling. However, the CNQX experiments also indicated that there must have been small miniature events which eluded detection. In a separate series of experiments, I estimated quantal size originated from synaptic vesicles resulted from evoked release by taking advantage of the variance-mean analysis, and overall results were consistent between variance-mean analysis and the analysis of mEPSCs.

Collectively, my results indicated that glutamate can leak out of vesicles unless it is continuously taken up from presynaptic cytosol. However, the magnitude of glutamate leakage was small and had only a minor effect on synaptic responses. In contrast, prominent rundowns of EPSC amplitude and mEPSC frequency observed after glutamate washout or Baf application are likely to be caused by accumulation of unfilled vesicles in presynaptic terminals retrieved after spontaneous and evoked glutamate release. I concluded that unlike isolated vesicles, glutamate leakage from synaptic vesicles in living synapses is limited, and there must be a mechanism to sustain glutamate in the lumen even in the absence of glutamate transport.

List of Figures

Fig 1-1. The schema of neuron	6
Fig 1-2. Synaptic transmission.....	6
Fig 1-3. Frog neuromuscular junction.....	8
Fig 1-4. Synaptic vesicle recycling	14
Fig 1-5. Vesicular neurotransmitter uptake	15
Fig 1-6. Characteristics of the functional synaptic vesicle pools.....	19
Fig 1-7. Leakage at equilibrium.....	24
Fig 2-1. Accessories for maintenance and mechanical fixation of slices	29
Fig 2-2. Patch clamp recording	31
Fig 2-3. The simultaneous whole-cell recordings	32
Fig 2-4. Detection of mEPSCs.....	37
Fig 3-1. Rundowns of EPSCs and mEPSCs after whole-cell washout of cytosolic glutamate in the presynaptic terminal.....	40
Fig 3-2. Rundowns of EPSCs and mEPSCs after block of glutamate uptake by bafilomycinA1	42
Fig 3-3. Reductions in the amplitudes of EPSCs and mEPSCs by CNQX titration.....	45
Fig 3-4. Exo-endocytic membrane capacitance changes in presynaptic terminals after glutamate washout	47
Fig 3-5. Nonstationary variance-mean analysis in the presence of glutamate.....	51
Fig 3-6. Nonstationary analysis in the presence of CTZ.....	52
Fig 3-7. Pharmacological reduction of quantal size by applying CNQX	54
Fig 3-8. mEPSC amplitude and quantal size estimated by nonstationary analysis after whole-cell washout of glutamate in the presynaptic terminal	58

1. Introduction

The aim of this thesis is to study the impact of neurotransmitter leakage from synaptic vesicles on synaptic transmission in physiological conditions. Therefore, I will start review the principles of neural signaling and synaptic transmission and then explain the rationale to study such phenomenon in this study.

1.1 Synaptic transmission

Neural networks consisting of neurons govern all aspects of brain functions, such as sensory cognition, motor control, learning and memory. A neuron is composed of a cell body, dendrites, and an axon (Fig 1-1). A cell body consists of the cytosol, the nucleus, mitochondria and other organelles. Dendrites usually receive numerous synaptic inputs and work as neural antennas. Axons have specialized structures for neural signal propagation. Neurons produce action potentials (APs), thereby conveying neural information. Hodgkin and Huxley revealed that APs are generated by a transient influx of sodium ions, followed by an efflux of potassium ions (Hodgkin and Huxley, 1952). Neural membranes are normally maintained at $-60\sim 80$ mV at rest. When a neuron is depolarized above the threshold of voltage-dependent sodium channel activation, an AP is generated. Essentially, sodium ions enter into the neuron through voltage-gated sodium channels according to an electrochemical gradient, and the membrane potential rises rapidly toward the sodium equilibrium potential ($\sim +50$ mV). This is soon followed by a fall of the membrane potential toward the potassium equilibrium potential (-100 mV) due to a subsequent opening of voltage-gated potassium channels.

Upon an arrival of APs at the presynaptic terminals, neurotransmitters stored in synaptic vesicles (SVs) are released to the synaptic cleft, a space between a presynaptic terminal and a postsynaptic cell, and reach specific receptors at the postsynaptic membrane, leading to their activation (Fig 1-2). There are two types of receptors for neurotransmitters. One is the ionotropic receptors whose activation results in an increase in the permeability of the membrane to certain ions. Ion influx through the receptors alters the membrane potential, thereby eliciting rapid signaling. Another is the metabotropic receptors which trigger activation of various intracellular signaling molecules such as GTP-binding proteins, thereby eliciting relatively slow responses. In case of the ionotropic receptors, whether they are excitatory or inhibitory depends on the charge of ions that they permeate to which direction. In the mammalian central nervous system, ionotropic glutamate receptors influx Na^+ , thereby depolarizing the membrane and triggering an excitatory postsynaptic potential (EPSP). Conversely, ionotropic GABA receptors allow influx of Cl^- , thereby hyperpolarizing the membrane and triggering inhibitory postsynaptic potentials (IPSPs). Likewise, the currents mediated by these ionotropic receptors can be measured as excitatory postsynaptic currents (EPSCs) and inhibitory postsynaptic currents (IPSCs) using the patch-clamp recording under the voltage-clamp mode (see the Chapter 2 for more details on the electrophysiological recording).

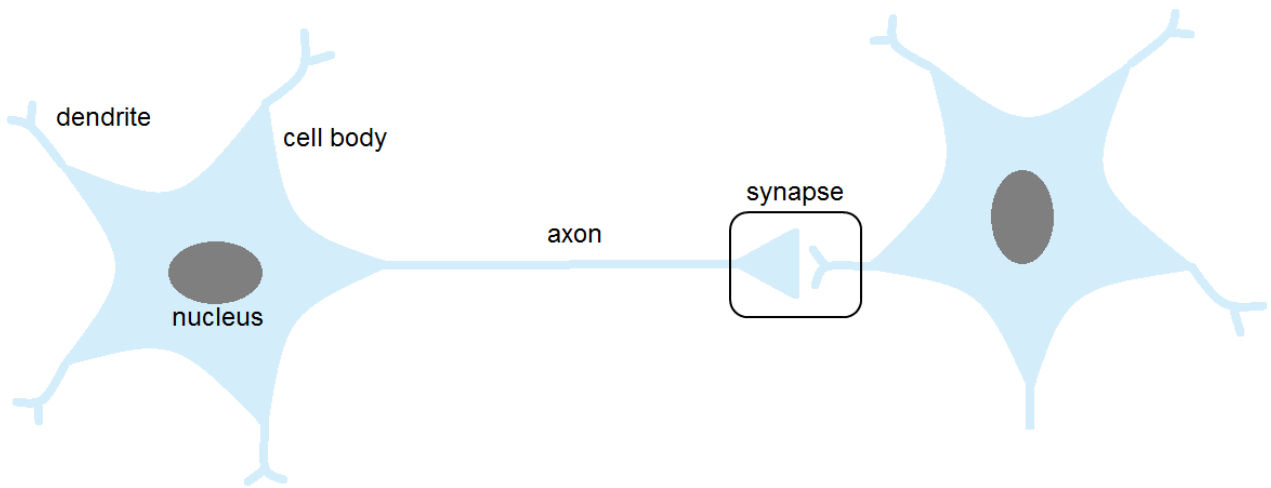


Fig. 1-1. The schema of neuron

A cell body of a neuron extends branches (dendrites) on which other neurons form synapses, and an axon that, in turn, make connections with other neurons

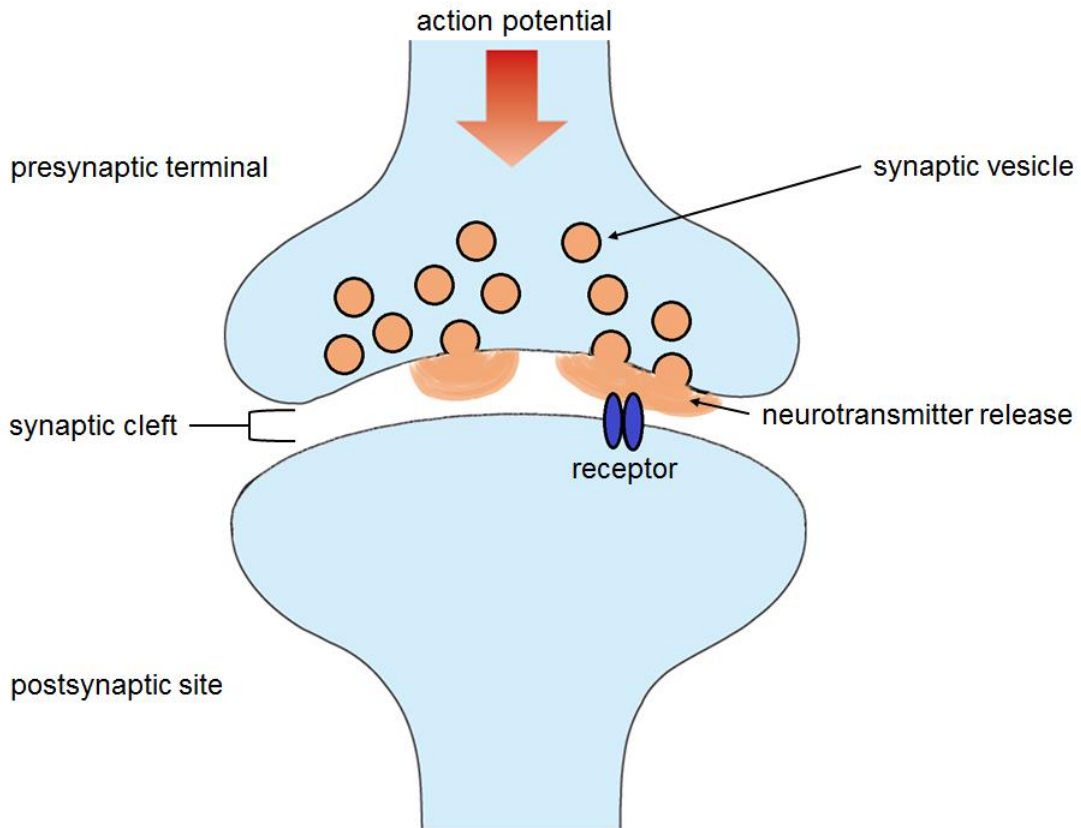


Figure 1-2. Synaptic transmission

Synapses are contact points between nerve cells or between nerve cells and their targets where signals are transmitted on from one cell to the next. At chemical synapses, the neurotransmitters released from the presynaptic terminal activate receptors in the postsynaptic membrane.

1.2. Parameters that determine the strength of neurotransmission

One of the most prominent features in neurotransmitter release is their quantal nature. Pioneering work by Katz and colleagues revealed that neurotransmitters are released as a shape of quantal packets of neurotransmitters (del Castillo and Katz, 1954; Katz and Miledi, 1969).

Fatt and Katz obtained the first clue as to the quantal nature of synaptic transmission when they made recordings from the neuromuscular junction (NMJ) of the frog without presynaptic stimulation and observed small spontaneous postsynaptic potentials of about 0.5 mV (Fatt and Katz, 1952). Because the synaptic potentials at vertebrate nervemuscle synapses are called end-plate potentials (EPPs), Fatt and Katz called these spontaneous potentials miniature EPPs (mEPPs). They reduced the amplitude of the evoked EPPs by lowering the extracellular calcium and adding extracellular magnesium. Under these conditions the responses fluctuated in a stepwise manner. Some stimuli produced no response at all; a failure of transmission. Some stimuli produced a response similar in size and shape to a mEPP. Others evoked responses that appeared to be two, three, or four times larger. This remarkable observation led them to propose the quantum hypothesis: that the single quantal events observed to occur spontaneously also represented the building blocks for the synaptic potentials evoked by stimulation.

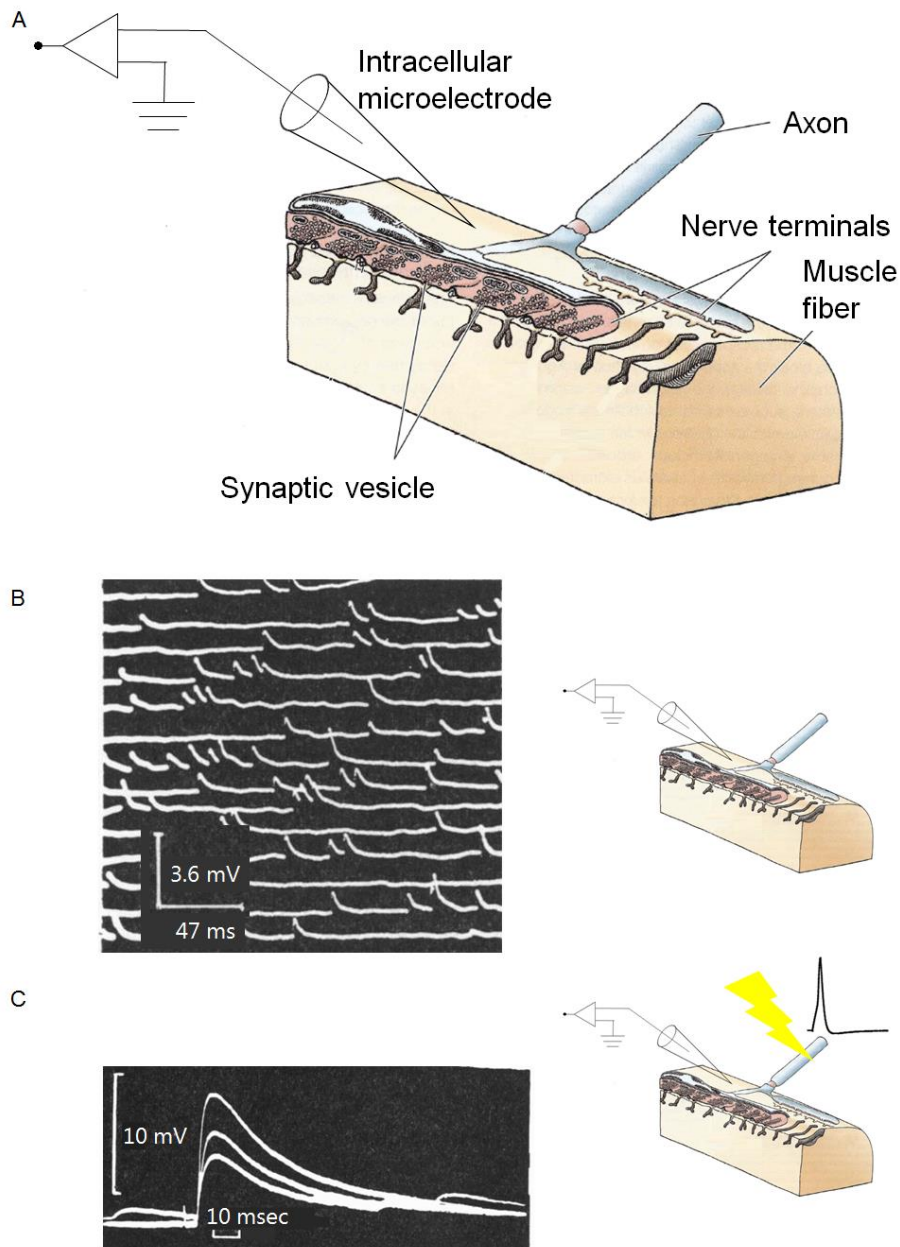


Fig1-3. Frog neuromuscular junction

A. A sketch of a terminal of a motor axon at the frog neuromuscular junction. Synaptic vesicles are clustered in the nerve terminal. B. miniature EPPs occur spontaneously and are confined to the end-plate region of the muscle fiber. C. presynaptic release of ACh was reduced by lowering the calcium concentration in the bathing solution. Sets of intracellular records, showing three superimposed responses to nerve stimulation, the amplitude of the EPP varies in a stepwise fashion. (Modified from "From Neuron to Brain fifth edition"; Fatt and Katz, 1952; del Castillo and Katz, 1954)

The quantum hypothesis was addressed by del Castillo and Katz using statistical analysis of the EPPs (del Castillo and Katz, 1954). When the NMJ is bathed in a solution low in calcium, all evoked

EPPs larger than the quantal synaptic potential are integral multiples of the unit potential. When the external calcium concentration is increased, the amplitude of the unit synaptic potential does not change. However, the number of failures decreases and the incidence of higher-amplitude responses increases. These observations demonstrate that alterations in external calcium concentration do not affect the size of a quantum of transmitter but rather affect the average number of quanta that are released in response to a presynaptic action potential.

Shortly after Katz and his colleagues demonstrated by electrophysiological methods that transmitter release was quantal, the electron micrographs of the NMJ revealed that axon terminals contain many small membrane-bound synaptic vesicles (Reger, 1958; Birks et al., 1960). Thus, it was suggested that a quantum of transmitter corresponds to the content of a single vesicle.

The amount of neurotransmitter released from presynaptic terminals is therefore determined by the number of available vesicles, the probability of the available vesicles to be released, and the amount of neurotransmitter in a vesicle. The strength of neurotransmission, which can be measured electrophysiologically as postsynaptic currents (PSCs), can be therefore described as the product of these parameters;

$$\text{PSCs} = N \times P_r \times q$$

where N , P_r , and q represent the number of release sites (or the number of vesicles available for release), release probability, and the quantal size, respectively (del Castillo and Katz, 1954). The quantal size is, unlike other parameters, defined by both the amount of neurotransmitters from a single vesicles and the sensitivity of postsynaptic receptors. This corresponds to the magnitude of the current

evoked at the postsynaptic membrane via ionotropic receptors activated by neurotransmitter released from a single SV, which is the miniature excitatory postsynaptic current (mEPSC) for excitatory synapses.

1.3. Synaptic vesicle recycling

Upon the arrival of action potentials, the voltage-dependent Ca^{2+} channels open and a transient calcium influx into the presynaptic terminals triggers exocytosis of SVs, and therefore discharge of neurotransmitters to the synaptic cleft. After exocytosis, SV constituents are retrieved by a process, called endocytosis. Newly formed SVs that are subsequently re-acidified and refilled with neurotransmitters undergo the next rounds of exocytosis (Fig 1-4). As such, SVs are recycled locally at the presynaptic terminals for sustained neurotransmission. In the following section, I will describe brief overview of current knowledge on SV recycling (Südhof and Rizo, 2011).

1.3.1. Exocytosis

Exocytosis of SVs is achieved by the cooperative actions of a number of intracellular proteins, principally by SNARE proteins that mediate the fusion between the vesicle membrane and the presynaptic plasma membrane (Jahn and Fasshauer, 2012; Südhof and Rizo, 2011). One SNARE protein, synaptobrevin/VAMP2 sits on the SV membrane (vesicle-or- v-SNARE), whereas two SNARE proteins called syntaxin 1 and SNAP-25 reside on the plasma membrane (target-or-r-SNARE). Their assembly is shown to be sufficient to promote membrane fusion by making two

opposing membrane close enough to merge *in vitro* (Weber et al., 1998).

Besides the SNARE proteins, synaptotagmin 1 and Munc-18 play important roles in synaptic vesicle fusion. Synaptotagmin 1 is a type I transmembrane protein which is expressed on the SV membrane and has low binding affinity to Ca^{2+} (Zhou et al., 2015). Multiple lines of evidence suggest that it is synaptotagmin 1 that synchronizes the activity-dependent Ca^{2+} influx through presynaptic Ca^{2+} channels to rapid exocytosis of SVs (Rizo et al., 2006). Although the mechanism of synaptotagmin 1 in Ca^{2+} -dependent exocytosis is not completely understood, it has been proposed that its interaction with both SNAREs and/or acidic phospholipids at the plasma membrane is involved (Chapman, 2008). Munc 18 in mice is a cytosolic protein, which was originally identified as a binding partner of syntaxin 1 (Hata et al., 1993). The precise action of Munc-18 in exocytosis is also unclear. However, the deletion of munc-18 in mice completely abolished exocytosis in neurons, indicating its pivotal role in neuronal exocytosis (Verhage et al., 2000).

In addition to SV proteins, scaffolding proteins at the active zone, a confined area at the presynaptic terminal where SV exocytosis occurs, such as RIMs (Wang et al., 1997; Wang et al., 2000), CAST, Bassoon and Piccolo (tom Dieck et al., 1998; Wang et al., 1999; Fenster et al., 2000), also contribute to regulate SV exocytosis, although many of them are not necessary but serve regulatory roles in exocytosis.

1.3.2. Endocytosis

After exocytosis, the components of the SV membrane are retrieved from the plasma membrane

and recycled into new SVs. At the classical endocytotic pathway, vesicles flatten completely into the plasma membrane following exocytosis, and vesicle constituents are retrieved via clathrin-coated pits (*clathrin-mediated endocytosis; CME*) (Heuser and Reese, 1973). Dynamin is critical for membrane fission of clathrin-coated vesicles from the presynaptic plasma membrane. After the fission, vesicles lose their coats to reform SVs and are refilled with transmitter. In contrast, following intense stimulation, a second pathway is activated in which vesicles pass through endosome-like structures that appear transiently in the cytoplasm. The endosomes are probably the result of direct retrieval of large pieces of membrane from the plasma membrane, which is called bulk endocytosis (Wu et al., 2007). Alternatively vesicles do not always collapse fully into the terminal membrane but instead form a transient fusion pore, after which they are recovered directly into the cytoplasm (kiss-and-run exocytosis). In this mode, vesicle contents are discharged partially or completely, depending on the size of the pore and duration of the pore opening (He et al., 2006; He et al., 2007). However, the presence of kiss and run mode of exocytosis is a matter of debate. Recently, “ultrafast endocytosis” has been proposed that is specialized to rapidly restore the surface area of the membrane (Watanabe et al., 2013). As will be discussed in the following section (‘Functional vesicle pool’), a time required for endocytosed vesicles to return to recycling vesicle pool would potentially limit the availability of vesicles for exocytosis at presynaptic terminals.

1.3.3. Re-acidification

After endocytosis, the activity of vacuolar-type H^+ ATPase (V-ATPase) generates an H^+

electrochemical gradient ($\Delta\mu_{H^+}$) across the SV membrane. The V-ATPase structurally resembles with mitochondrial F_0F_1 -ATP synthase. Like the F_0F_1 -ATP, it consists of a peripheral V_1 domain which is responsible for ATP hydrolysis and an integral V_0 domain which is responsible for H^+ transport (Marshansky et al., 2014). Whereas F_0F_1 -ATP synthase is an enzyme that produces ATP molecules by using an H^+ electrochemical gradient across the mitochondrial membrane, the V-ATPase does the opposite task. The $\Delta\mu_{H^+}$ consists of two components; a chemical gradient (ΔpH) and a membrane potential ($\Delta\Psi$). Since the V-ATPase is an electrogenic pump, shunting ionic currents are needed for sufficient transport of protons. In synaptic vesicles, Cl^- is a candidate for this shunt, thus promoting ΔpH rather than $\Delta\mu\Psi$, although molecular identify of the Cl^- permeation has been enigmatic. It is also known that SVs contain cation/ H^+ exchanger that essentially dissipates ΔpH . Since the proportion of $\Delta\Psi$ and ΔpH has impact on neurotransmitter loading into synaptic vesicles (see below), changes in activities of these enigmatic ion transporters on synaptic vesicles might regulate neurotransmitter contents.

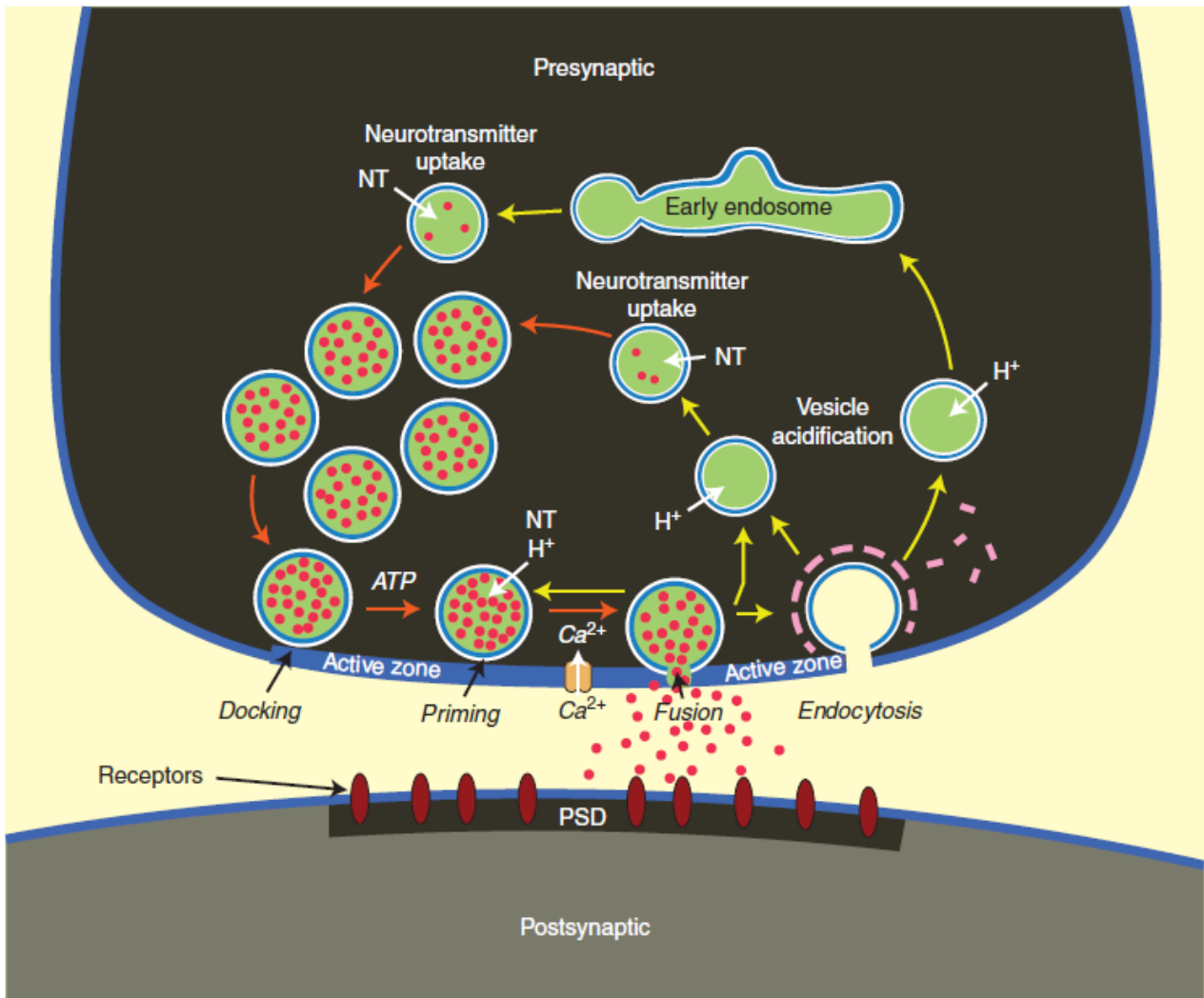


Figure 1-4. Synaptic vesicle recycling (modified from Südhof and Rizo, 2011)

Before synaptic exocytosis, SVs are docked at the active zone, and primed via an ATP-dependent process. Following calcium influx through voltage-gated calcium channels, they undergo exocytosis and release neurotransmitter to the synaptic cleft. Exocytosis occurs at release sites mainly within specialized areas of the presynaptic membrane, called active zones, which are defined by their spatial proximity to voltage-activated calcium channels and by the presence of scaffolding proteins. Endocytosis of SV membranes occurs within the periactive zone that surrounds the active zone area. SV endocytosis is predominantly mediated by a clathrin- and dynamin-dependent pathway. Kiss-and-run mode of exocytosis has been postulated, though a matter of debate. Newly-endocytosed SVs are energized by the activity of the V-ATPase that drives neurotransmitter refilling into SVs for the next round of exocytosis.

1.3.4. Vesicular neurotransmitter uptake

Unlike plasma membrane neurotransmitter transporters that utilize Na^+ gradient across the plasma

membrane, uptake of neurotransmitters into synaptic vesicles depends on a H^+ electrochemical gradient ($\Delta\mu_{H^+}$) that is generated by the V-ATPase. A relative requirement of the two components of $\Delta\mu_{H^+}$ ($\Delta\Psi$ or ΔpH) for the uptake of neurotransmitter depends on the charge of the substrate. Uptake of positively-charged transmitters such as monoamine and acetylcholine depends predominantly on ΔpH , whereas that of negatively charged transmitters such as glutamate depends on $\Delta\Psi$. Uptake of zwitter-ionic transmitters such as GABA and glycine depends equally on both of the components (Fig 1-5) (Edwards, 2007).

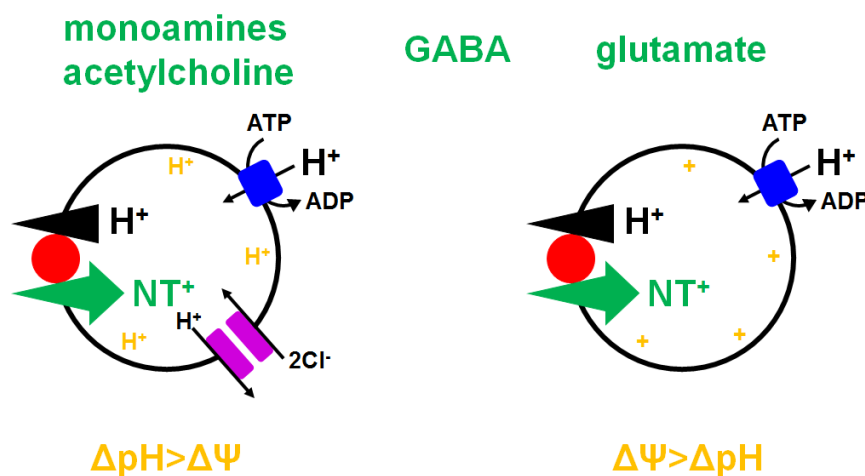


Figure 1-5. Vesicular neurotransmitter uptake (Modified from Edwards, 2007)

The movement of H^+ down their electrochemical gradient is coupled to the transport of transmitter in the opposite direction. Despite this common H^+ exchange mechanism, different vesicular neurotransmitter transporters rely to differing extents on the two components of the H^+ electrochemical gradient, the chemical gradient ΔpH and the electrical gradient $\Delta\Psi$. Vesicular monoamine and ACh transport, which involves the exchange of protonated cytosolic transmitter for two luminal H^+ , involves more H^+ than charge movement and hence depends more on ΔpH than $\Delta\Psi$. Conversely, transport of negatively charged glutamate depends more on $\Delta\Psi$ than ΔpH . Transport of the zwitterion GABA with no net charge equally depends on both ΔpH and $\Delta\Psi$.

In consistent with distinct bioenergetics of the vesicular transporters, there are five transporter families that are structurally distinct, vesicular monoamine transporter1/2 (VMAT1/2), vesicular acetylcholine transporter (VACHT), vesicular glutamate transporter1~3 (VGLUT1~3), vesicular GABA/inhibitory amino acid transporter (VGAT/VIAAT), and vesicular nucleotide transporter (VNUT) (Omote and Moriyama, 2013). In the following paragraph, I will focus on the VGLUTs, since the preparations that I used throughout the study were glutamatergic synapses that utilize VGLUTs for vesicle refilling.

The VGLUTs belong to the solute carrier (SLC) 17 family that includes the type I phosphate transporter. VGLUT1 and VGLUT2 were originally identified as plasma membrane inorganic phosphate transporters. In fact, heterologous expression of the proteins conferred Na⁺-dependent Pi uptake activity to xenopus oocytes. However, they were localized preferentially to synaptic vesicles of seemingly glutamatergic neurons in rodent brains and the expression of these proteins conferred an ability to transport glutamate into intracellular acidic compartments. Although transport properties, such as substrate specificity and affinity of VGLUT1 and VGLUT2 were indistinguishable, VGLUT1 and 2 show a mutually exclusive distribution in the mammalian CNS (Fremeau et al., 2004). VGLUT1 is strongly expressed in the cerebral cortex and hippocampus, whereas VGLUT2 is expressed in the thalamus, brainstem, and deep cerebellar nuclei. In the cerebellum, parallel fiber express VGLUT1, whereas climbing fiber terminals express VGLUT2 (Fremeau et al., 2002). Indistinguishable from the wild type at birth, VGLUT1 knockout (KO) mice older than 2 to 3 weeks fed poorly and do not survive unless cared individually. After weaning, they can survive

independently for several months, but show progressive neurological phenotypes that included blindness, incoordination, and an enhanced startle response (Fremeau et al., 2004; Wojcik et al., 2004).

VGLUT2 KO mice die at birth that demonstrates the importance of VGLUT2 in early development and its predominance in the brainstem and pons, in which the neurons controlling the basic functions of respiration and the autonomic nerve system reside (Moechars et al., 2006; Wallen-Mackenzie et al., 2006).

VGLUT3 is expressed in a small population of neurons that were not considered as glutamatergic neurons. VGLUT3 KO mice showed subtle global deficiencies, although they were found to be deaf due to the degeneration of inner hair cells in the organ of Corti (Seal et al., 2008).

1.4. Functional vesicle pools

Not all synaptic vesicles clustered at the presynaptic terminals are constantly engaged in vesicle recycling. Rather, vesicles are divided into three functionally distinct vesicle pools; a readily releasable pool (RRP), a recycling pool, and a reserve pool (Rizzoli and Betz, 2005). Synaptic vesicles in the RRP are immediately available on stimulation. These vesicles are generally thought to dock at the presynaptic active zone, and prepared for immediate release ("primed"). Vesicles in the recycling pool maintain release during relatively mild stimulation. This pool is thought to contain about 5~20 % of all vesicles that are continuously recycling to sustain transmitter release. The reserve pool is defined as a depot of synaptic vesicles from which release is only triggered during intense stimulation. These vesicles constitute the majority (typically 80~90 %) of vesicles in most presynaptic terminals.

These distinct vesicle pools have been investigated using techniques such as electrophysiology and electron and fluorescence microscopy. The main characteristics of the vesicles pools in two preparations, rodent cultured hippocampal neurons and rodent calyx of Held neurons in slice preparation, are summarized below.

In cultured hippocampal neurons, the total vesicles population in each bouton comprises 100~200 vesicles (Schikorski & Stevens, 1997). A RRP in this type of synapses, consisting of only 5~20 vesicles, is experimentally defined as vesicles released by hypertonic shock, indicating that they are adjacent to the plasma membrane and fully primed (Rosenmund and Stevens, 1996). A recycling pool comprises 10~20 % of the vesicles (Harata et al., 2001), and the rest represents the resting pool. In contrast, a giant calyx of Held presynaptic terminal contains a much larger number of vesicles, approximately ~200,000 in total (de Lange et al., 2003). At postnatal day (P) 8~11, the RRP consists of ~ 2,500 vesicles (Sakaba and Neher, 2001) and the recycling pool consists of ~10,000 vesicles (Fig 1-5) (de Lange et al., 2003). Interestingly, inhibition of cyclin-dependent kinase 5 (CDK5), a kinase implicated in neural development and signaling, strongly shifted a portion of the reserve pool to the recycling pool, leading to a presynaptic potentiation (Kim and Ryan, 2010). Thus, functional vesicle pool is inter-changeable depending on the usage, and therefore contributing to various types of presynaptic regulation in the physiological and pathological context.

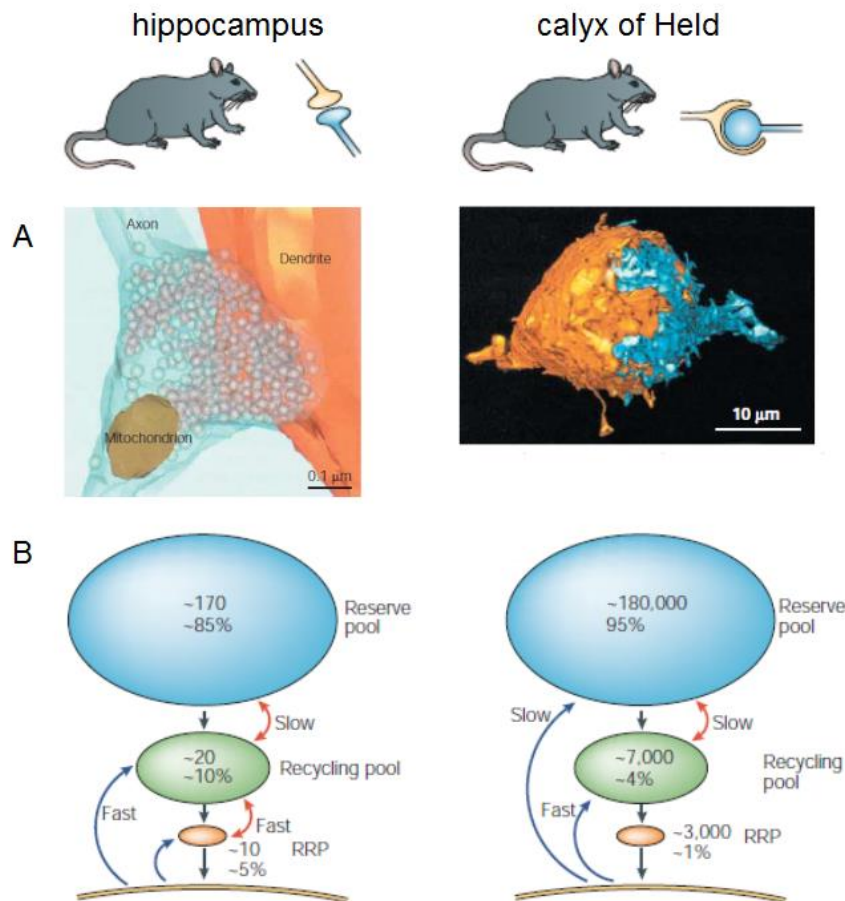


Fig. 1-6. Characteristics of the functional synaptic vesicle pools. (Modified from Rizzoli and Betz, 2005)

Left is a typical image of the rat cultured hippocampal synapse, and right is that of the rat calyx of Held synapse. A. Three dimensional reconstruction (left; a bouton. Right; presynaptic terminal in orange and postsynaptic cell in blue.) B. Pool size and mixing rates. Blue arrows indicate endocytosis and red arrows indicate mixing between pools.

1.5. Presynaptic regulation of quantal size

Classically, it has been considered that the amount of neurotransmitters in individual vesicles is constant and not regulated under physiological conditions. However, this notion has not been tested due to the lack of suitable experimental techniques and in-depth quantitative analyses. In this thesis, I attempted to develop such techniques and analyses to better understand whether neurotransmitter leak can occur. This would fill our knowledge gap in the synaptic physiology and provide insights into the sustainability and energetics of the presynaptic machinery. In the following sections, I will

briefly discuss current knowledge and concepts in respect to the presynaptic regulation of quantal size with special focus on glutamatergic synapses.

1.5.1. Cytosolic neurotransmitter concentrations

Biochemical assays using isolated SVs have suggested that the rate of substrate transport as well as the amount of substrates accumulated into vesicles depend on the transmitter concentration in the cytosol (Naito and Ueda, 1985; Maycox et al., 1988). In case of glutamatergic synapses, physiological cytoplasmic glutamate concentrations are estimated to be 3~5 mM at the calyx of Held (Ishikawa et al., 2002). Neurotransmitter glutamate is synthesized locally at the presynaptic terminal from glutamine by the activity of phosphate-activated glutaminase (PAG), therefore the expression of PAG might play important roles in glutamatergic transmission. However, basal glutamatergic transmission was intact in PAG-knockout mice, indicating other synthetic pathways for neurotransmitter glutamate (Masson et al., 2006).

Impacts of presynaptic glutamate concentration on synaptic transmission was directly investigated using the calyx of Held synapses as a model (see also below (1.6. Calyx of Held)). In support with *in vitro* observations, loading of high concentration of glutamate into the presynaptic terminal via whole-cell dialysis resulted in marked enhancement of EPSC (Ishikawa et al., 2002; Yamashita et al., 2003). On the other hand, glutamate washout from the presynaptic terminals caused a gradual rundown of EPSCs, collectively indicating that cytosolic glutamate concentrations might affect the quantal size (Ishikawa et al., 2002; Hori and Takahashi, 2012).

1.5.2. Regulation of the driving force

Since vesicular neurotransmitter transporters are secondary transporters that critically depend on the driving force supplied by the V-ATPase, changes in the driving force might have a substantial impact on the rate and the amount of transmitters transported into vesicles. As explained in 1.3.4, the contributions of either $\Delta\Psi$ or ΔpH on transmitter uptake vary depending on transmitters and the balance of two components is regulated mainly by extravesicular (cytosolic) Cl^- concentrations (Edwards, 2007). In case of positively charged transmitters such as monoamines and acetylcholine, high concentrations of Cl^- facilitates ΔpH , resulting in larger uptake. In contrast, glutamate uptake exhibits an unusual Cl^- dependency (Naito and Ueda, 1985): Uptake is most efficient at medium Cl^- concentration but becomes sub-maximal at high or low concentrations. While attenuation of transport by high concentration of Cl^- may be explained by the reduction of $\Delta\Psi$, the transport activity is also reduced at low Cl^- concentrations. The reason for this biphasic effect of Cl^- on glutamate transport has been enigmatic, and direct activation of VGLUTs by Cl^- ions has been proposed (Bellocchio, 2000). Whatever the mechanism is, the biphasic Cl^- dependency of glutamate uptake was recapitulated in the calyx of Held synapses, where glutamate transport into vesicles were assessed under various cytosolic Cl^- concentrations (Hori and Takahashi, 2012). Contributions of cytosolic cations on quantal size of glutamate were also demonstrated in the calyx of Held. In consistent with biochemical observations that cation/ H^+ exchanger expressed on SVs enhances $\Delta\Psi$ in the expense of ΔpH , removal of K^+ from the terminals attenuate glutamate release, presumably due to reduced $\Delta\Psi$ (Goh et al., 2011). Furthermore, Na^+ influx into the terminals via HCN channels during intense

stimulations caused an increase of quantal size (Huang and Trussell, 2014).

1.5.3. Transporter expression

Increase in the expression of transporters on vesicles would, theoretically, affect the transport rate rather than the final concentration of transmitter in the lumen. However, overexpression of vesicular transporters in various preparations resulted in increase of transmitter contents. For instance, overexpression of VGLUT1 in hippocampal neurons caused a significant increase in the mEPSC amplitudes (Wojcik et al., 2004; Wilson et al., 2005), indicating an increase of the quantal size. Consistently, the remaining mEPSCs in VGLUT1 knockout neurons were significantly smaller than those in wild-types neurons (Wojcik et al., 2004). Moreover, in drosophila mutants that overexpress drosophila VGLUT (DVGLUT) in motor neurons exhibited an increase in the quantal size (Daniels et al., 2004). In the latter case, increase in the vesicular volume was evident, implying a possible mechanism for the increased quantal size. Despite the clear evidence for the enhanced quantal size by the increased transporter expression, other work suggested that expression levels of VGLUTs do not affect quantal size. First, neurons derived from VGLUT1-heterozygous knockout mice that express ~ 50 % of VGLUT1 compared to wild-type did not display any changes in mEPSC amplitudes (Wojcik et al., 2004; Fremeau et al., 2004). Also, neuromuscular junctions of drosophila mutants that expressed minimum levels of DVGLUT exhibited only reduction in a frequency of miniature events but not in their amplitudes (Daniels et al., 2006). Currently, there is no coherent model that can explain all the observations described above.

1.5.4. Leakage at equilibrium

The amount of transmitters in a vesicle might be set at a balance between active transport via the transporters and passive leakage either via reverse transport or via non-specific leakage through the membrane. Indeed, isolated vesicles from rat brains lost their contents (glutamate and GABA) during purification process, which could be prevented when the V-ATPase was kept working (Burger et al., 1989), indicating a pathway for leakage. However, since the vesicle isolation required relatively long time (several hours to 2 days), contributions of the transmitter leakage on synaptic transmission during a short period remained unclear.

With *in vitro* assays, relatively fast glutamate leakage (< several min) from vesicles was observed only when vesicles were imposed to pharmacological manipulations that selectively dissipated ΔpH after glutamate transport reached at equilibrium (Wolosker et al., 1996). Furthermore, when vesicle acidification was monitored in the presence of glutamate uptake, an addition of bafilomycin A₁ (Baf), the specific inhibitor of the V-ATPase, caused a fast alkalization whose kinetics was distinct from that of vesicles pre-acidified by Cl⁻ (Hnasko et al., 2010). These observations supported a concept that glutamate can leak out of vesicles once the driving force was modulated.

In contrast to *in vitro* assays, application of Baf to neural preparations resulted in somewhat contradicting observations. By using hippocampal cultured neurons, Zhou et al. demonstrated that mEPSC amplitudes were slightly reduced after a long incubation with Baf (Zhou et al., 2000). In parallel, the frequency of miniature events was dramatically reduced, leaving a possibility that miniature events from partially-filled vesicles had eluded detection. Conversely, another study using

autaptic cultures derived from hippocampus demonstrated that Baf application did not reduce mEPSC amplitudes at all (Ikeda and Bekkers, 2009). The gradual EPSC rundown after a brief Baf application was, therefore, explained solely by accumulation of empty recycling vesicles that had released their content by exocytosis. One of the intrinsic problems using Baf to block glutamate refilling was that Baf is a membrane permeable reagent that may also produce unexpected effects on properties of synaptic membranes such as the permeability, stability, and lipid dynamics. Indeed, it was demonstrated that Baf induced a rapid increase in release probability during application, which may cause a rapid depletion of some recycling vesicle pools (Zhou et al., 2000), contributions of which had not been considered carefully in the previous analysis. Thus, it is still controversial whether neurotransmitter can leak out of SVs in native nerve terminals.

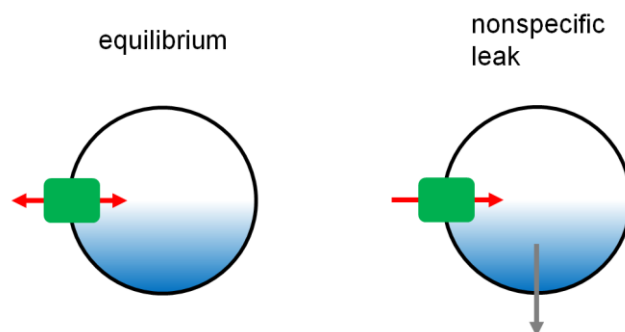


Fig 1-7. Leakage at equilibrium (Modified from Edwards, 2007)

There are two possible pathways for neurotransmitter leakage from SVs. Left: At equilibrium, the ionic coupling of vesicular neurotransmitter transporters together with the H^+ electrochemical driving force should dictate the direction transmitter movements through the respective transporters. Right: Depending on properties of neurotransmitters, there is a nonspecific leak through vesicle membranes which is not mediated by the neurotransmitter transporters.

1.6. Aim of this work

Glutamate leakage from SVs can directly alter the quantal size and could be one of the critical determinants of synaptic transmission. However, characterizing the leak pathway and its mechanism has been proven difficult in living neurons due to the lack of techniques. Instead of the pharmacological blockade of the V-ATPase, previous work in Takahashi's laboratory has taken advantages of the giant calyx of Held synapses, in which cytosolic glutamate could be dialyzed through a patch pipet to minimize glutamate refilling into newly-formed SVs specifically. Although unexpected side effects of the mechanical membrane rupture and the dialysis of cytosolic components indispensable for synapse functions could not be completely ruled out, this manipulation provided an alternative method to track glutamate leakage from preloaded vesicles.

Interestingly, glutamate washout caused rundown of the EPSC and mEPSC amplitudes, similar to that under Baf application (Zhou et al., 2000), but the magnitudes of rundown differed between EPSCs and mEPSCs, with a steeper decline in the evoked EPSC amplitudes (Ishikawa et al., 2002; Wu et al., 2007). One of the explanations for such a difference was that, as described above for Baf experiments, leakage of glutamate from synaptic vesicles can increase the number of undetectable events which could not be detected beyond the background noise. Alternatively, as shown in the previous studies, contributions of spontaneously fusing vesicles between stimulation pulses on the rundown of the evoked EPSCs (assuming that the same vesicle pool is used both for spontaneous release and activity-dependent exocytosis) were not carefully considered to explain faster rundown of the evoked EPSCs. In other words, spontaneous events accumulate empty vesicles and one does

not have to assume leakage of glutamate from synaptic vesicles.

In this thesis, I attempted to clarify impact of glutamate leakage on quantal size regulation by analyzing the quantal size during glutamate washout from the presynaptic terminals of the calyx of Held. First, I performed a series of experiments to clarify whether, and to what extent, glutamate can leak out of vesicles during glutamate washout by monitoring mEPSCs under minimum stimulation conditions. Next, I attempted to examine whether glutamate washout would alter quantal size during high frequency stimulation. For this purpose, I developed a novel analytical method, by which quantal sizes during evoked release could be estimated.

1.7. Calyx of Held

Throughout this study, I used the calyx of Held synapses as a model synapse. The calyx of Held is a giant nerve terminal located in the auditory brainstem, superior olivary complex. Auditory signals arriving at the cochlea are transmitted to the ipsilateral anterior ventral cochlear nucleus by excitatory synapses onto globular and spherical bushy cells. The axons of globular bushy cells cross the brainstem midline and make a synaptic contact onto the principal cells of the contralateral medial nucleus of the trapezoid body (MNTB). These myelinated axons have a large diameter, allowing a fast conduction velocity, and give rise to the calyx of Held. Thanks to their exceptionally large structures, various molecules can be directly loaded into the calyx of Held via whole-cell patch pipettes, while simultaneous recording from both the presynaptic terminal and the postsynaptic cell are possible (Hori et al., 1999; Takahashi et al., 2000). Although calyx of Held is large, electron

microscopic studies revealed that individual active zones, which are separated by 0.4 μm (Meinrenken et al., 2002), resemble those of small conventional synapses found in other regions of the mammalian CNS (Lenn and Reese, 1966). Throughout its postnatal developmental period, a single calyx synapse express both VGLUT1 and VGLUT2, and they exhibit segregated localizations within the synapse (Billups, 2005).

The large size of the presynaptic terminal allows us to remove cytosolic glutamate through the patch pipettes, which cannot be done in conventional synapses such as those in cultured hippocampal preparation. In addition, because the terminal makes a synapse directly onto the postsynaptic soma, postsynaptic events such as EPSCs and mEPSCs could be reliably measured using voltage clamp. We took advantage of this unique preparation to measure the impact of glutamate washout and address the issue of glutamate leakage on synaptic transmission in the present study.

2. Materials and Methods

2.1. Ethical approval

All experiments were performed in accordance with the guideline of the Physiological Society of Japan and Doshisha University, and were approved by the local committee for handling experimental animals in Doshisha University.

2.2. Preparation of slices for patch clamp experiments

2.2.1. Slicing

C57BL6 mice at postnatal day (P) 12- to -15 were deeply anaesthetized by inhalation of isoflurane (Wako Chemicals, Japan) and killed by decapitation prior to rapid dissection of the brain. This procedure took within 1~1.5 min. The tissue was kept cold throughout sectioning, thereby presumably minimizing damage from anoxia and improving the texture of the tissue for slicing. For this purpose, the tissue was submerged in ice-cold cutting solutions (mM): 234 sucrose, 2.5 KCl, 1.25 NaH₂PO₄, 10 MgCl₂, 0.5 CaCl₂, 26 NaHCO₃, 11 glucose (nacalai tesque, Japan). Mechanical stability of the tissue is essential for making thin slices. For this purpose, the brainstem containing the calyx of Held-MNTB region was cut by hand. A surface of this block, trimmed parallel to transverse of the slices, was glued to the stage of the slices. The slicing chamber was immediately filled with physiological saline and surrounded with ice while slicing. A vibrating microslicer (VT1200S, Leica, Germany) was used to cut slices of 175 μ m thickness. After sectioning, each slice was immediately placed in oxygenated artificial cerebrospinal fluid (aCSF) containing (mM): 125 NaCl, 2.5 KCl, 26 NaHCO₃,

1.25 NaH₂PO₄, 2 CaCl₂, 1 MgCl₂, 10 glucose, 3 myo-inositol, 2 sodium pyruvate, and 0.5 ascorbic acid (pH 7.3 with 95% O₂, 5% CO₂, 310 mosmol/kg) at 37°C, where it remains until use. In order to ensure efficient oxygenation and continuous movement of the solution, the slices were bubbled directly from below. A method using simple disposable accessories is illustrated in Fig 2-1.

2.2.2. Mechanical fixation for recording

One slice at a time was placed in the glass bottomed recording chamber and held in place with a grid of parallel nylon thread (Fig2-1). Such a grid, placed over the slice, held it firmly in position on the bottom of the recording chamber.

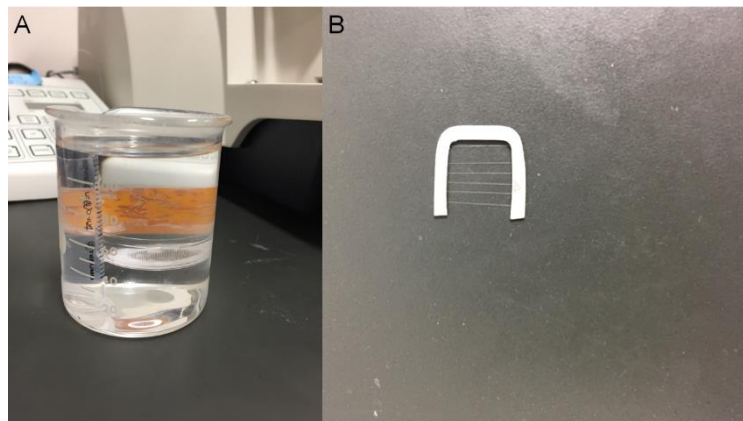


Figure 2-1. Accessories for maintenance and mechanical fixation of slices.

A. Maintenance of slices following sectioning. A holding chamber is placed on top of a 50 ml beaker. A suitable chamber is made by breaking the top and bottom out of a small plastic Petri dish, forming two rings. The ring formed from a lid is made so that, when inverted, it fits tightly onto the lip of the base. A piece of fine cotton mesh is stretched over the ring made from the base and can be clamped in place by the ring made from the lid. B. Grid for mechanical fixation of the slice during recording, the slice is fixed on the bottom of the recording chamber by a grid of nylon threads glued to a platinum frame.

2.2.3. Optical setup

An upright microscope (Axioskop, Carl Zeiss, Germany) with Nomarski optics was used to see the upper surface of the slice. Two changes have been made to the microscope which make recording easier. The focusing mechanism has been altered to move the objective instead of the stage. A hinge has been added to the microscope frame so that the top half of the microscope can be tipped back making it much easier to place the patch pipettes in position in the bath. The objective is an Achromat 60× water immersion lens (LUMPlanFI, Olympus, Tokyo) with a working distance of 1.6 mm. For improved visibility when using thicker slices, a black and white television camera was attached to the microscope via an adapted phototube. All procedures were then observed on a screen.

2.3. Whole-cell patch clamp recordings

2.3.1. Whole-cell recording

The patch clamp technique offers an increased resolution in the recording of currents across cell membrane. The development of the patch clamp by Neher, Sakmann, and their colleagues, has made an enormous contribution to the knowledge of the functional behavior of membrane channels (Hamill et al., 1981). Patch clamp recordings involve sealing the tip of a small (1 μm internal diameter) glass pipette to the membrane of a cell. Patch pipettes were pulled from borosilicate glass (GC150F-10, HARVARD APPARATUS, UK). The pipettes are pulled using a micropipette puller (MODEL P-97, Sutter Instrument, USA) and standard Nichrome heating coils supplied with it. In the pull, the capillary is thinned to obtain a tip diameter of 1~5 μm. Due to the small working distance (1.6 mm)

of the water immersion objective, the pipette approached the neurons at a low angle ($\sim 15^\circ$ to the horizontal plane). Under ideal condition, with slight suction on the pipette, a seal resistance of greater than $10\text{ G}\Omega$ is formed around the rim of the pipette tip between the cell membrane and the glass. In this thesis, I used the whole-cell recording configuration in which I applied slight additional suction to rupture the membrane inside the patch, thereby providing access to the cell cytoplasm (Fig2-2).

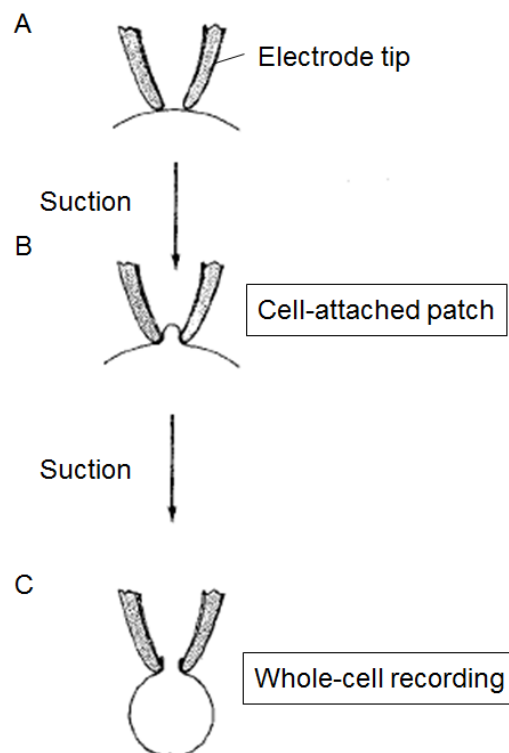


Figure 2-2. Patch clamp recording

Patch configurations are represented schematically. The electrode forms a seal on contact with the cell membrane (A), which is converted to a gigaohm seal by gently suction (B). The membrane within the electrode tip may be ruptured by further suction to obtain a whole-cell recording (C) (modified from Hamill et al., 1981).

2.3.2. Simultaneous pre- and postsynaptic recordings

Simultaneous pre- and postsynaptic recordings from calyces of Held and the MNTB principal cells were made in the presence of $100\ \mu\text{M}$ picrotoxin to block GABA_A receptors, $0.5\ \mu\text{M}$ strychnine to

block glycine receptors and D (-)-2-amino-5-phosphonopentanoic acid (D-AP5, 50 μ M) to block N-methyl-D-aspartate receptors (Fig2-3).

Whole-cell recordings from calyx of Held and MNTB cells were made with an Axopatch 700A amplifiers. The postsynaptic pipette solution contained (mM): 140 CsCl, 40 Hepes, 5 EGTA, 1 MgCl₂, 5 QX-314 (pH 7.3, 320 mosmol/kg). The presynaptic pipette solution contained (mM): 100 K methanesulfonate, 30 KCl, 40 Hepes, 0.5 EGTA, 12 phosphocreatine (Na salt), 3 ATP (Mg salt), 0.5 GTP (Na salt), 0 or 3 K glutamate (pH 7.3, 310-320 mosmol/kg). The postsynaptic pipette was pulled to 5-7 M Ω and had a series resistance of 10-25 M Ω , which was compensated by up to 75% for a final value of 7 M Ω . The resistance of the presynaptic pipette was 7-10 M Ω , and series resistance was typically 14-20 M Ω , which was not compensated. When the postsynaptic series resistance increased by > 15 M Ω during recording, data were discarded. The postsynaptic holding potential was -70 mV. The liquid junction potential between pipette and external solution was not corrected. In simultaneous presynaptic and postsynaptic recordings, EPSCs were evoked by presynaptic action potentials elicited by a 1 msec depolarizing pulse (Takahashi et al., 1996).

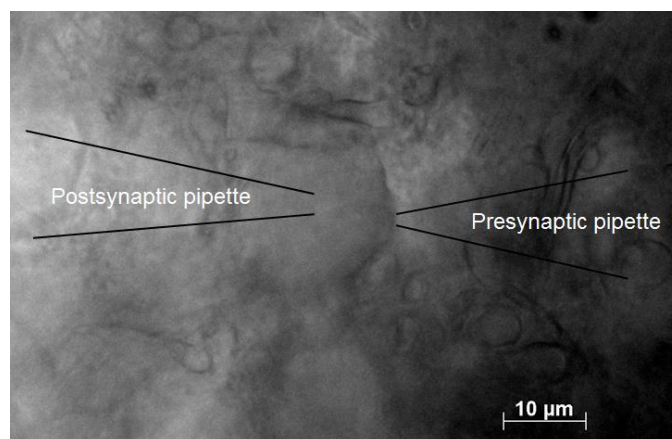


Figure 2-3. The simultaneous whole-cell recordings
The simultaneous whole-cell recordings from the calyx of Held (right) and MNTB principle cell (left).
Glass pipettes are patched to the calyx of Held and MNTB from both sides.

2.4. Capacitance measurement

Fusion of synaptic vesicles with the plasma membrane leads to a transient increase of membrane surface area, soon followed by a surface decrease corresponding to endocytosis. These changes in the cell surface area can be followed by monitoring the electrical capacitance of the cell. The starting point is a conventional whole-cell patch clamp recording, which can be modeled electrically by an access resistance in series with the parallel membrane resistance and capacitance. The circuit parameters in the model are typically estimated by applying sinusoidal command voltages to the patch pipette and by analyzing the resulting currents (Lindau and Neher, 1988).

Membrane capacitance measurements were made from calyx of Held presynaptic terminals in whole-cell configuration at room temperature (Yamashita et al. 2010; Eguchi et al. 2012). Calyceal terminals were voltage-clamped at a holding potential of -80 mV and a sinusoidal voltage command with a peak-to-peak voltage of 60 mV was applied at 1 kHz. The presynaptic pipette solution contained (mM): 125 Cs-methanesulfonate, 30 CsCl, 10 HEPES, 0.5 EGTA, 12 Na₂-phosphocreatine, 3 MgATP, 1 MgCl₂, 0.3 Na₂GTP, 0 or 3 Cs-Glutamate (pH 7.3, 315-320 mosmol/kg). Single-pulse step depolarization (to +10 mV, 10 ms) was used to induce presynaptic I_{Ca}. Membrane capacitance (C_m) changes within 450 ms of square-pulse stimulation were excluded from analysis to avoid contamination by conductance-dependent capacitance artifacts (Yamashita et al, 2005). To avoid the influence of capacitance drift on baseline, we discarded data when the baseline drift measured 0-10 s before stimulation was > 5 fF/s. When the capacitance baseline drift was 1-5 fF/s, we subtracted a linear regression line of the baseline from the data for the baseline correction.

Data were acquired at a sampling rate of 100 kHz, using an EPC-10- patch-clamp amplifier controlled by PatchMaster software (HEKA Elektronik) after on-line filtering at 5 kHz. The recording pipette was pulled to 5-7 M Ω and had a series resistance of 9-14 M Ω , which was compensated by up to 50 % for a final value of 7 M Ω . Care was taken to maintain series resistance < 14M Ω to allow diffusion of drugs into the terminal.

For recording presynaptic Ca²⁺ currents, the aCSF contained 10 mM tetraethylammonium chloride, 0.5 mM 4-aminopyridine, 1 μ M tetrodotoxin, 10 μ M bicuculline methiodide and 0.5 μ M strychnine hydrochloride.

The postsynaptic pipette solution contained (mM): 140 CsCl, 40 Hepes, 5 EGTA, 1 MgCl₂, 5 QX-314 (pH 7.3, 320 mosmol/kg). The presynaptic pipette solution contained (mM): 100 K methanesulfonate, 30 KCl, 40 Hepes, 0.5 EGTA, 12 phosphocreatine (Na salt), 3 ATP (Mg salt), 0.5 GTP (Na salt), 0 or 3 K glutamate (pH 7.3, 310-320 mosmol/kg).

2.5. Variance-mean analysis

Various forms of fluctuation analysis have been used in the past to estimate the quantal parameters, including N (number of release sites), P_r (release probability) and q (quantal size) (Silver *et al.* 1998; Clements & Silver, 2000; Meyer *et al.* 2001). They are all based on the quantal theory, according to which the average evoked EPSC peak amplitude (I) is,

$$I = N \times P_r \times q \tag{1}$$

Knowing q , the quantal content (M) is readily obtained from:

$$M = N P_r = I/q \quad (2)$$

Assuming binomial statistics, the variance (σ^2) of evoked EPSC peak amplitudes can be written as:

$$\sigma^2 = Nq^2 P_r (1 - P_r) \quad (3)$$

Dividing σ^2 by I yields:

$$\sigma^2/I = q(1 - P_r) \quad (4)$$

If release probability were extremely low ($P_r \ll 1$), q can, thus, be approximated from the variance of evoked EPSC peak amplitudes divided by their mean amplitude (σ^2/I).

For analysis, a suitable stretch of repetitively applied trains with sufficiently stable whole-cell parameters (R_s and leak current) was used. I applied a stimulation protocol consisting of 200 trains of 10 stimuli at 200 Hz, and repeated 30 times with a 100 msec intervals. Total stimulation period is 30 sec at this protocol. At the calyx of Held synapses, long lasting trains of stimuli induce noticeable synaptic depression, which has been proposed to result from depletion readily releasable pool. The release probability might be low during train ($P_r \ll 1$). In addition, a 100 msec interval between trains courses partial recovery from synaptic depression which developed during 200 Hz train stimulation. To estimate quantal size during high frequency stimulation, the mean EPSC amplitudes and the variance of EPSC amplitudes were analyzed for last 30 trains. The mean amplitude of EPSCs and the variance of EPSCs are plotted on a graph, and slopes of variance–mean plots were estimated by linear regression.

2.6. Analysis of electrophysiological data

Signals were low-pass filtered at 5 kHz and digitized at 20 kHz with Digidata 1322A using pClamp 8 acquisition software (Molecular Devices).

2.6.1. Detection of mEPSCs with a scaled template

mEPSCs can be difficult to detect when their amplitudes are close to the background noise. For detecting mEPSCs, I used a sliding template method implemented in Axograph. The templates were made by initially averaging 50-150 mEPSCs selected manually. A waveform with the time course of the template was slid along the current or voltage trace and optimally scaled to fit the data at each position. The decay of averaged mEPSC was fitted by double exponential functions, and its weighted mean time constant (τ_m) was calculated from individual time constants (τ_1 , τ_2) and their relative amplitude (a_1 , a_2) as follows: $\tau_m = a_1\tau_1 + a_2\tau_2$.

A detection criterion was calculated from the scaling factor and the quality of the fit. An event was detected when this criterion crosses a threshold level. Overlapped mEPSCs were excluded from analyses by visual inspection.

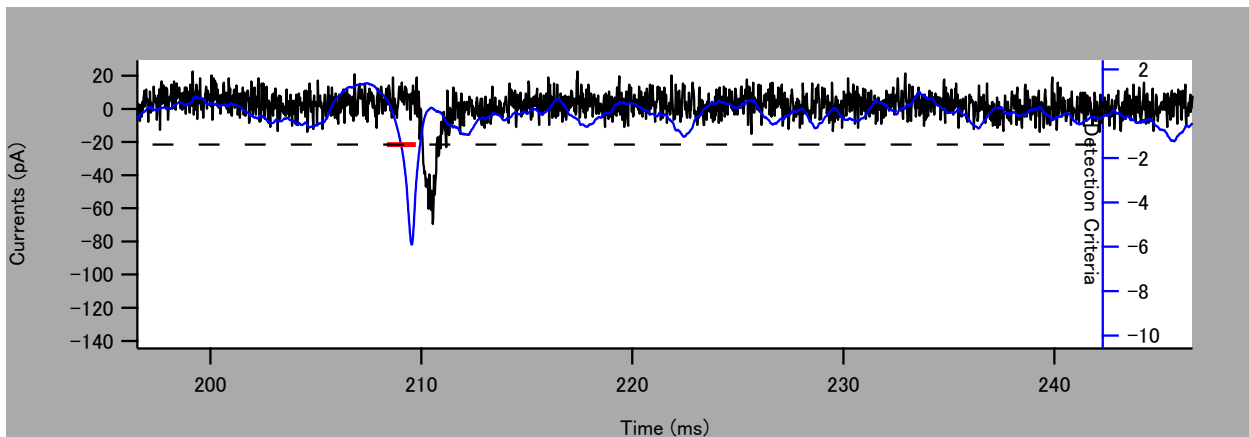


Figure 2-4. Detection of mEPSCs

A detection criterion, calculated from the optimally scaled template, was used to detect small synaptic events. A simulated data trace containing one mEPSC superimposed on recording noise. The mEPSC is 60 pA in amplitude and occur at 210 ms. A template with the same time course as the synaptic events (0.5 ms rise, 0.6 ms decay time constant), was stepped along the record. The detection criterion exhibits a sharp negative going peak when the template is optimally aligned with a synaptic event. With the detection threshold set to -1.4 (*dashed line*).

2.6.2. mEPSC amplitude compensation

In the CNQX experiments, the mEPSC frequency should be constant even if CNQX concentration has a graded increase. However, mEPSC frequency decreased in proportion to mEPSC amplitudes. This indicates that undetectable quantum increases with the mEPSC decreasing. The decreasing percentage of mEPSC frequency consists with undetectable quantum. In the glutamate washout experiments, the relationship between mEPSC frequency and undetectable quantum refer to the following table (modified from Fig 3-3D).

Normalized mEPSC frequency (Normalized EPSC amplitude)	The number of undetectable quantum/ total synaptic vesicle number of exocytosis
0.2	0.5
0.4	0.4
0.6	0.3

In the glutamate washout experiments, the decreasing percentage of mEPSC frequency consists with

that of EPSC amplitude.

At the variance-mean analysis, I compensated the mEPSC amplitude assuming that undetectable mEPSC amplitudes were 0 pA.

2.7. Statistical analysis

All statistical analyses were performed using IBM-SPSS 24-software (SPSS Inc., Chicago, IL, USA).

The effects of glutamate washout were analyzed by a repeated-measures ANOVA with glutamate concentrations ([Glu]: 3mM, 0mM) as between-subjects factor and time (0, 10, 20, 30 min after glutamate washout) as within-subjects factor. The effects of Baf were equally analyzed by a repeated-measures ANOVA with drug (DMSO, Baf) as between-subjects factor and time (before drug application, 0, 10, 20, 30 min after drug application) as within-subjects factor. Bonferroni tests were used for *post hoc* comparisons. All data were expressed as mean \pm S.E.M.

3. Results

3.1. Washout of presynaptic cytosolic glutamate

Glutamate is concentrated in synaptic vesicles at 60-150 mM (Burger et al. 1989) by vesicular glutamate transporters (VGLUTs; Takamori et al. 2000; Bellocchio et al. 2000) using trans-vesicular proton gradient produced by the V-ATPase (Naito & Ueda, 1985). Endogenous cytosolic glutamate concentration in presynaptic terminals is estimated to be 1-10 mM at the calyx of Held in different postnatal periods (Ishikawa et al. 2002; Yamashita et al. 2009). In simultaneous whole-cell recordings from a calyx of Held presynaptic terminal and a postsynaptic MNTB neuron in slices of mice brainstem, I dialyzed presynaptic terminals with a glutamate-free pipette solution (Ishikawa et al. 2002; Yamashita et al. 2009; Hori & Takahashi, 2012). I then evoked EPSCs every 10 min (Fig. 3-1) and meanwhile recorded spontaneous mEPSCs, which represent quantal, or single vesicular, EPSCs at this synapse (Sahara & Takahashi, 2001). After glutamate washout, EPSCs decreased in amplitude with a time constant of 22 min, whereas mEPSC amplitude underwent a less significant decline with a tendency to reach a plateau (Fig. 3-1B). These results are similar to those reported by Ishikawa et al. (2002), where EPSCs are evoked at 0.1 Hz. During glutamate washout, mEPSC frequency significantly decreased from 33 ± 12 Hz to 3.6 ± 2.0 Hz (n=5 pairs) in 30 min (Fig. 3-1C). In control experiments, when glutamate was included in the presynaptic pipette at 3 mM, no significant change was observed in the mean amplitude of EPSCs, mEPSCs or the mean frequency of mEPSCs. The number of vesicles undergoing spontaneous exocytosis during glutamate washout was estimated as $24,700 \pm 6,700$ (n=5 pairs). This number could be an underestimate, because empty vesicles due to

glutamate washout should be added to this number. Thus, fast rundown of EPSCs can be explained, at least in part, by increased number of empty vesicles involved in EPSCs.

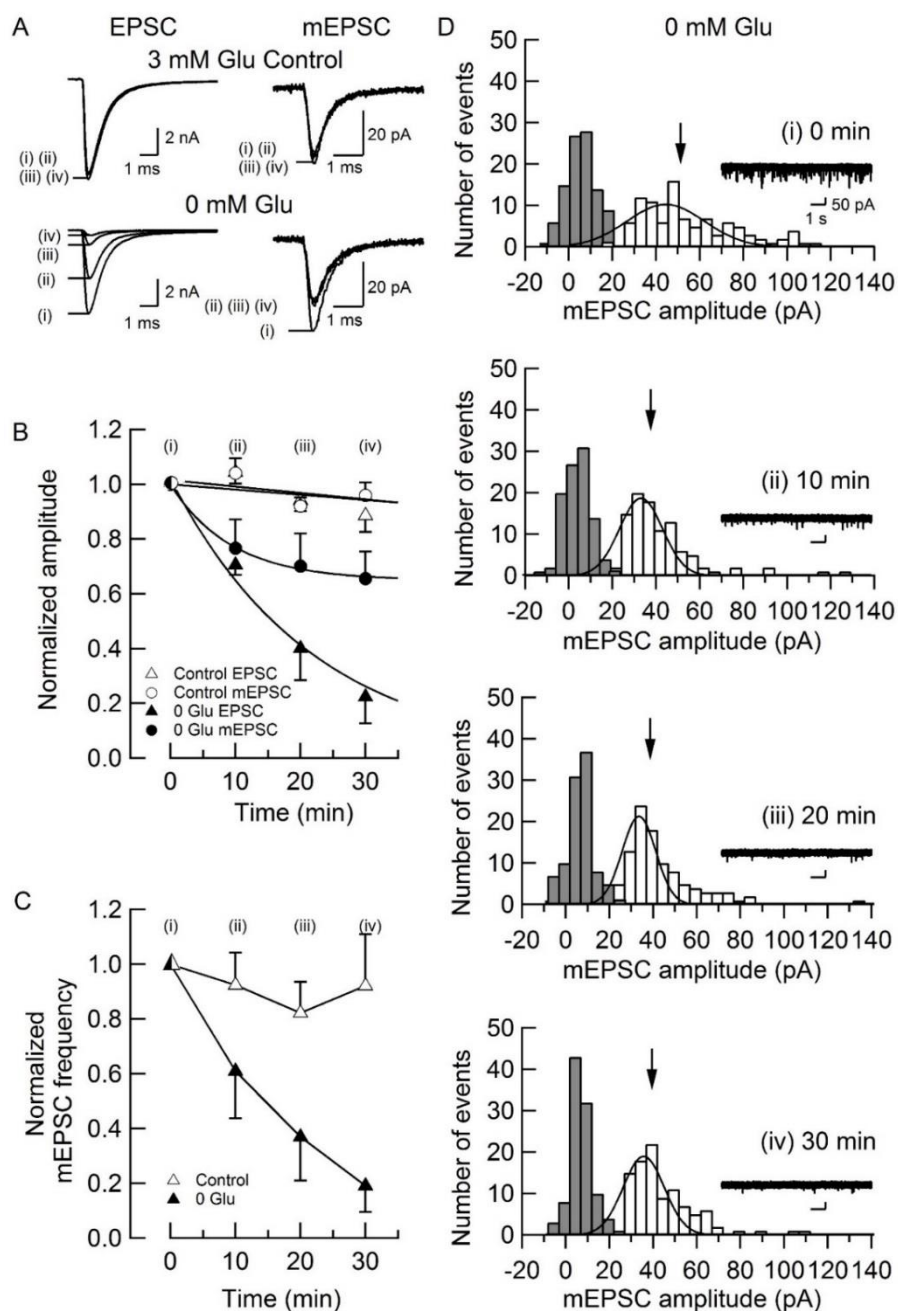


Fig 3-1. Rundowns of EPSCs and mEPSCs after whole-cell washout of cytosolic glutamate in the presynaptic terminal.

A. Sample traces of EPSCs and mEPSCs, before and 10-30 min after glutamate washout (lower traces, superimposed), and controls with 3 mM glutamate in presynaptic pipettes (upper traces). B. Mean amplitudes of EPSCs (triangles) and mEPSCs (circles) at different time periods after glutamate washout (filled symbols) or controls with 3 mM glutamate (open symbols). Each data derived from five experiments and normalized to the mean amplitudes at time 0 just after rupturing presynaptic membrane (ordinate). Error bars indicate + or - SEMs in this and following Figures. Exponential curves were best fit

to data points with an equation of $I=I_0 + (1 - I_0)e^{-\frac{t}{\tau}}$, where the time constant (τ) and I_0 was 22 min and 0, respectively for EPSCs, whereas 9.4 min and 0.65, respectively for mEPSCs. At time 0, mean amplitudes of evoked EPSCs was 7.5 ± 0.5 nA (3 mM Glu control, n=5 pairs) and 7.8 ± 0.7 nA (0 mM Glu, n=5 pairs) and those of mEPSCs was 35 ± 1.4 pA (3 mM Glu control, n=5 pairs) and 43 ± 7.2 pA (0 mM Glu, n=5 pairs). Glutamate concentrations ([Glu]) had significant effects on the amplitude of mEPSCs (repeated-measures ANOVA: main effect of [Glu]: $F_{1,8} = 5.03$, $P > 0.05$; main effect of time: $F_{3,24} = 8.3$, $P < 0.001$; [Glu] \times time interaction $F_{3,24} = 4.2$, $P < 0.05$) and that of EPSCs (repeated-measures ANOVA: main effect of [Glu]: $F_{1,7} = 31$, $P < 0.001$; main effect of time: $F_{1,4,10} = 35$, $P < 0.001$; [Glu] \times time interaction $F_{1,4,10} = 18$, $P < 0.001$). Miniature EPSC amplitudes between 0 min and 30 min without glutamate in presynaptic pipettes were significantly different (Bonferroni tests: $P < 0.05$). The difference in rundown magnitude between controls with 3 mM glutamate and those without glutamate was statistically significant for EPSCs at 10 min, 20 min and 30 min (Bonferroni tests: $P < 0.01$). C. Mean frequency of mEPSCs at different time periods after glutamate washout, normalized to the mean frequency at time 0. The mean frequency of mEPSCs at time 0 was 17 ± 1.3 Hz (3 mM Glu control, n=5 pairs) and 15 ± 4.2 Hz (0 mM Glu, n=5 pairs). Glutamate concentration had significant effects on the frequency of mEPSCs (repeated-measures ANOVA: main effect of [Glu]: $F_{1,8} = 7.4$, $P < 0.05$; main effect of time: $F_{3,24} = 9.7$, $P < 0.001$; [Glu] \times time interaction $F_{3,24} = 5.4$, $P < 0.05$). Statistical difference between controls and 0 mM glutamate was significant at 20 min (Bonferroni tests: $P < 0.05$) and 30 min (Bonferroni tests: $P < 0.01$). D. Representative amplitude histograms of mEPSCs (open bars) at different time periods after glutamate washout. Traces in inset show mEPSCs at a slow time scale in this Figure and Figure 2C. Total number of events is 100 for each histogram. Background noise distributions (filled bar) were obtained from the baselines of records with no clear mEPSC events. Arrows indicate mean amplitude of mEPSCs in this Figure and Figure 2. Gaussian curves are fit to mEPSC amplitude histograms using the least-square method. The coefficient of variation (c.v.) of mEPSC amplitudes was 0.47, 0.52, 0.45, and 0.40, respectively for 0, 10, 20 and 30 min after glutamate washout.

3.2. Block of vacuolar ATPase with bafilomycin A1

To make a direct comparison with previous studies possible, I bath-applied the V-ATPase blocker bafilomycin A₁ (Baf in DMSO, 5 μ M for 100 s, Fig. 3-2) in intact synapses without presynaptic whole-cell recording, as previously reported at cultured hippocampal synapses (Ikeda & Bekkers, 2009). In control experiments, I bath-applied DMSO alone (0.5 %). Within 5 min after Baf application (100 s), the mEPSC amplitude started to decline and remained similar thereafter, whereas the EPSC amplitude and mEPSC frequency continuously declined. These results are consistent with those by

Zhou et al. (2000), but inconsistent with those by Ikeda & Bekkers (2009), reporting that the mean amplitude of mEPSCs does not change after Baf application. Just after Baf application, there was a transient increase in mEPSC frequency (Fig. 3-2C). Together with the previous report showing a transient increase in EPSC amplitude and a decrease in the paired-pulse ratio seen just after Baf application at cultured hippocampal synapses (Ikeda & Bekkers, 2009), Baf likely has a side effect causing a transient increase in the release probability.

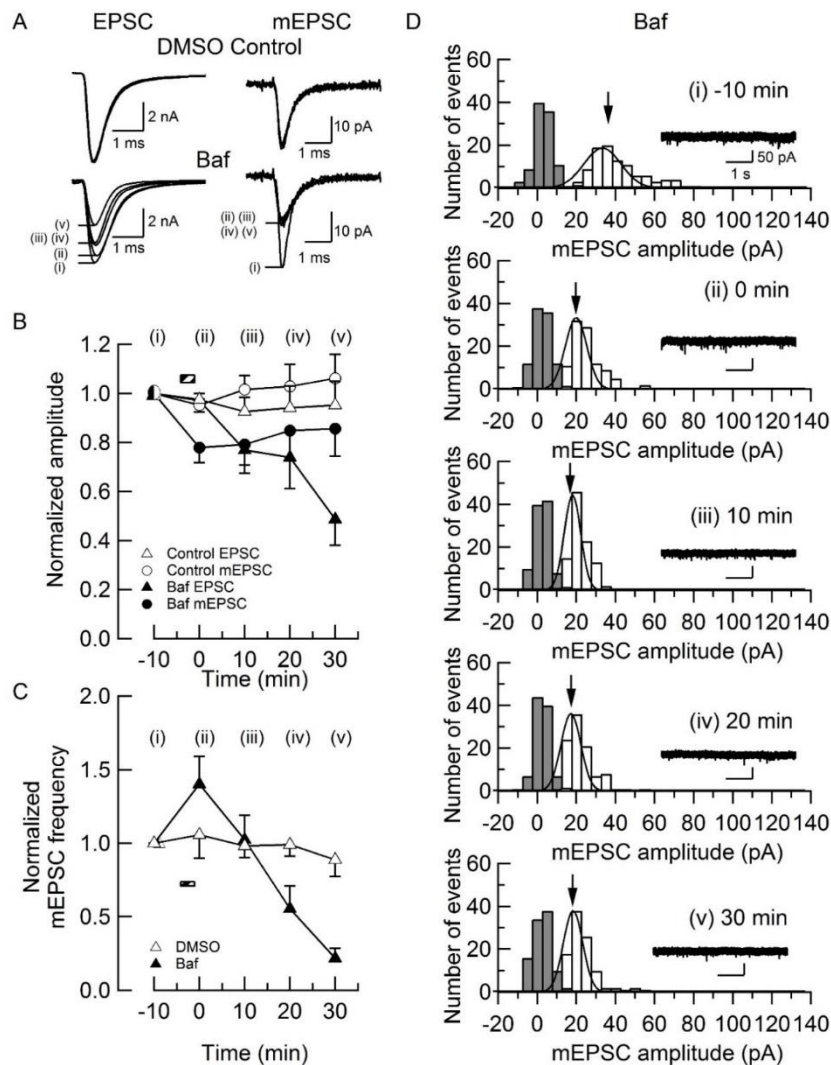


Fig 3-2. Rundowns of EPSCs and mEPSCs after block of glutamate uptake by bafilomycin A1.

A. Sample traces of EPSCs and mEPSCs before and 0-30 min after 100 s bath-application (hatched box) of Baf ($5 \mu\text{M}$ with 0.5% DMSO, lower traces, superimposed), or DMSO alone (controls, upper traces).

Presynaptic terminals were kept intact without whole-cell recording. B. Mean amplitudes of EPSCs (triangles) and mEPSCs (circles) at different time periods after application of Baf (filled symbols) or DMSO alone (open symbols). Each data derived from five experiments and normalized to the amplitudes before applying Baf or DMSO. The mean amplitude of evoked EPSCs before drug application was 7.3 ± 0.8 nA (DMSO, n=5 cells) and 7.5 ± 0.6 nA (Baf, n=8 cells) and that of mEPSCs was 38 ± 5.5 pA (DMSO, n=5 cells) and 38 ± 3.7 pA (Baf, n=8 cells). Drug application had a significant effect on the amplitude of mEPSCs (repeated-measures ANOVA: main effect of drug: $F_{1,11} = 6.0$, $P < 0.05$; main effect of time: $F_{2,24} = 2.2$, $P > 0.05$; [Glu]×time interaction $F_{2,24} = 2.3$, $P > 0.05$) and that of EPSCs (repeated-measures ANOVA: main effect of drug: $F_{1,8} = 8.1$, $P < 0.05$; main effect of time: $F_{4,32} = 16$, $P < 0.001$; [Glu]×time interaction $F_{4,32} = 13$, $P < 0.001$). Differences in the magnitude of amplitude reduction between DMSO controls and Baf application data was statistically significant for mEPSCs at 0 min (Bonferroni tests: $P < 0.05$) and EPSCs at 30 min (Bonferroni tests: $P < 0.01$). C. Mean frequency of mEPSCs at different time periods after application of Baf (filled triangles) or DMSO alone (open symbols) normalized to the initial values before drug application. The mean frequency of mEPSCs before drug application was 5.6 ± 1.4 Hz (DMSO, n=5 cells) and 8.7 ± 2.0 Hz (Baf, n=8 cells). Drug application had a significant effect on the frequency of mEPSCs (repeated-measures ANOVA: main effect of drug: $F_{1,11} = 0.8$, $P > 0.05$; main effect of time: $F_{4,44} = 13$, $P < 0.001$; [Glu]×time interaction $F_{4,44} = 8.0$, $P < 0.001$). Miniature EPSC frequency was significantly reduced at 0, 10, 20 and 30 min after Baf application (Bonferroni tests: $P < 0.05$). D. Representative amplitude histograms of mEPSCs (open bars) at different time periods after Baf application. Total number of events is 100 for each histogram. The c.v of mEPSC amplitudes was 0.28, 0.25, 0.27, 0.23 and 0.35, respectively for before and 0, 10, 20 and 30 min after applying Baf.

3.3. mEPSCs reduced by CNQX.

The reduction of mEPSC amplitude after glutamate washout or Baf application suggested that glutamate leaks out of vesicles when glutamate uptake is blocked. However, the small rundown of mEPSC amplitude with a following plateau after Baf application in cultured hippocampal synapses has been ascribed to a low detectability of mEPSCs (Zhou et al. 2000). To validate this possibility, I tested the effect of postsynaptic AMPA receptor block on mEPSC amplitudes by applying CNQX at incremental concentrations (0.2 ~ 1.5 μ M, Fig. 3-3). As CNQX concentration increased, the mean amplitudes of EPSCs and mEPSCs declined in parallel (Fig. 3-3B). At 1.5 μ M CNQX, mEPSCs were still detectable above the noise level (Fig. 3E), with a mean amplitude of 19 ± 0.8 pA (n=5 pairs), that

is ~40 % of control size. This mean amplitude was significantly smaller than that measured after glutamate washout for 30 min (26 ± 3.0 pA, n=5 pairs, $P < 0.05$) or after Baf application (27 ± 3.5 pA, n=5 cells), indicating that mEPSCs after rundown were well above the detection limit of mEPSCs. Although AMPA can depolarize calyceal presynaptic terminals (Takago et al. 2005), CNQX by itself at $1.5 \mu\text{M}$ had no effect on presynaptic membrane potential (n = 4 cells, data not shown), excluding its presynaptic effect.

Notably, the reduction of mEPSC amplitude by CNQX was associated with a decline of mEPSC frequency (Fig. 3-3C). This is likely due to the secondary effect of amplitude reduction, with small events merging into the noise. For a given reduction of mEPSC amplitude, the percentage reduction of mEPSC frequency was less in CNQX application than in glutamate washout (Fig. 3-3D), suggesting that the reduction of mEPSC frequency after glutamate washout was caused primarily by accumulation of empty vesicles and secondarily by an increase of undetectable events associated with a reduction of mEPSC amplitude.

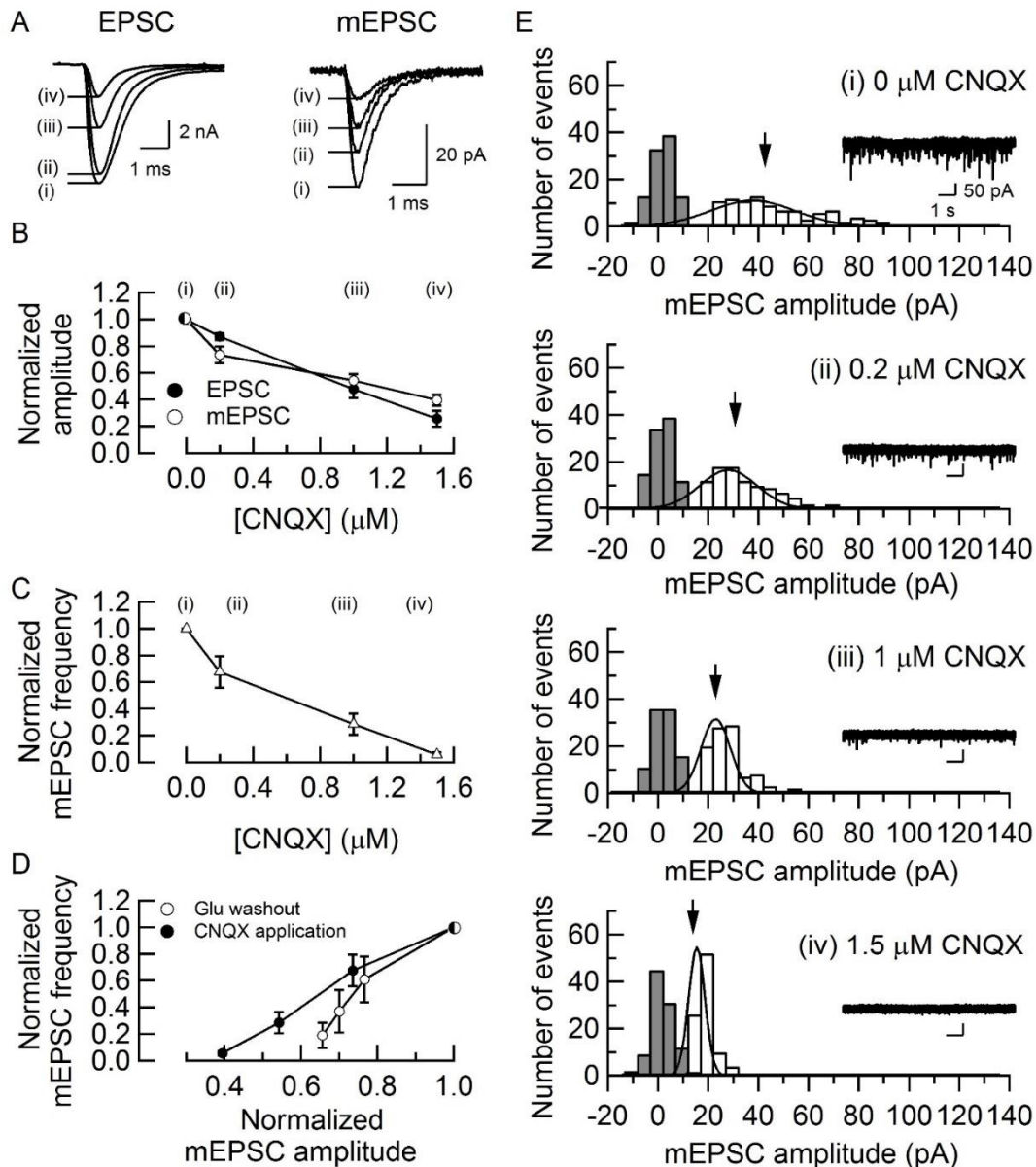


Fig 3-3. Reductions in the amplitudes of EPSCs and mEPSCs by CNQX titration.

A. Sample traces of EPSCs and mEPSCs without or with CNQX at different concentrations (0.2-1.5 μM , superimposed). B. Mean amplitudes of EPSCs (filled circles) and mEPSCs (open circles) plotted against CNQX concentrations. Each data was derived from five experiments and normalized to controls without CNQX (ordinate). In the presence of 1.5 μM CNQX, the mean amplitude of evoked EPSCs was 2.1 ± 0.5 nA and that of mEPSCs was 19 ± 0.8 pA. C. Mean frequency of mEPSCs in the presence of CNQX at different concentrations, normalized to control. D. Relative mEPSC frequency (ordinate) plotted against relative mEPSC amplitude during glutamate washout (open circles) and in the presence of CNQX at different concentrations (filled circles). E. Amplitude histograms of mEPSCs recorded from a postsynaptic neuron in the presence of CNQX at different concentrations. The c.v of mEPSC amplitudes was 0.44, 0.43, 0.32 and 0.23, respectively in the presence of 0, 0.2, 1.0, 1.5 μM CNQX.

3.4. Influence of filling state on vesicle recycling

However, the reduction of mEPSC frequency may also indicate reduced release probability. At hippocampal autaptic culture preparations, the vesicular neurotransmitter filling state is proposed to regulate exocytosis, with poorly filled vesicles having a low release probability (Herman et al. 2014). To examine whether the greater reduction of EPSC amplitude than that of mEPSC amplitude after glutamate washout (Fig. 3-1B) might be caused by a reduction of release probability, we measured membrane capacitance of calyceal presynaptic terminals (Sun et al. 2002; Yamashita et al. 2005) during glutamate washout. If release probability declines, exocytic capacitance change (ΔC_m) is expected to decrease. However, ΔC_m remained unchanged during glutamate washout (Fig. 3-4). Furthermore, no change was discerned for the presynaptic Ca^{2+} currents or the time course of endocytic capacitance change (Fig. 3-4B), suggesting that presynaptic glutamate washout has no effect on exocytosis or endocytosis of synaptic vesicles. These results are consistent with those of unchanged FM dye de-staining after Baf application in cultured hippocampal synapses (Zhou et al, 2000), as well as with those of similar membrane capacitance changes, with or without intracellular glutamate, in *Salamander* retinal cells (Bartoletti & Thorenson, 2011). Taken together, the results suggest that the reduction of mEPSC frequency results from the accumulation of empty vesicles in the absence of cytoplasmic glutamate.

3.5. Quantal size can be monitored during high frequency stimulation by the non-stationary variance-mean analysis.

So far, I have shown the estimation of quantal size in a vesicle by measuring mEPSC events. However, as evident from Fig. 3-3D, there must have been small miniature events which eluded detection. In order to detect all quantal events including these small ones, I intended to measure the quantal size during evoked synaptic transmission. A standard way to estimate the quantal size during an evoked response was originally developed by Silver and colleagues (Silver et al., 1998), in which quantal parameters were mathematically estimated from the fluctuation of evoked EPSCs recorded from rat climbing fiber-Purkinje cell synapses. Practically, EPSCs were recorded under various release probabilities by altering extracellular Ca^{2+} concentrations. From a plot of the variance of the EPSC amplitudes with the mean of them, quantal size (q) as well as number of release sites (N) and release probability (P_r) in each condition could be determined. This variance-mean analysis could be applied to the calyx of Held-MNTB synapse (Koike-Tani et al., 2008). However, since this experimental procedure requires relative long recording periods including a successive stimulation for at least 20 min, the same stimulation protocol cannot be applied repetitively to monitor the effect of glutamate washout during 30 min.

Subsequently, Meyer and colleagues modified the variance-mean analysis in which alterations of release probabilities are achieved via synaptic depression upon high frequency firing (Meyer et al., 2001). This analysis using evoked responses at the initial phase of synaptic depression was proven to

reliably estimate quantal parameters as the original method, but the recording still required for 10 ~ 15 min.

To perform a variance-mean analysis to estimate the quantal size during glutamate washout, I applied a stimulation protocol consisting of 200 trains of 10 stimuli at 200 Hz with the inter-train interval of 100 ms. At this synapse, trains of stimuli induce noticeable synaptic depression, which has been proposed to result from the depletion of the readily releasable pool (Meyer et al., 2001). Fig 3-5 shows results from one of such recordings. The plot of the average EPSC amplitude of the 1st pulse in each train (Fig 3-5B) revealed that the train stimuli induced robust synaptic depression. The first EPSCs in train 1 had an average amplitude of 6.62 ± 0.73 nA ($n=4$), whereas the average amplitude of the 10th EPSCs in train 1 was depressed to 32 ± 2.9 %. The EPSC amplitude of the 1st pulses in the following train slightly recovered from depression during the 100 ms interval, presumably as a result of replenishment of vesicles from the reserve pool. The responses reached a plateau at the last 30 trains, due to a putative balance between the depletion and the replenishment of the readily-releasable pool. To estimate the quantal size during high frequency stimulation, the mean EPSC amplitudes and the variance of EPSC amplitudes were analyzed for the last 30 trains. When the variance of EPSCs during the last 30 trains was plotted against the corresponding average EPSC amplitudes, the initial slope of a linear fitting gave a quantal size of $q = 31 \pm 3.5$ pA, which was reasonable within the range of quantal sizes reported previously (Sahara and Takahashi, 2001).

It is known that, after activation, the AMPA-type glutamate receptors enter a desensitized state in which glutamate remains bound but the receptor channel is closed. I wondered whether the

desensitization of the receptors during the high frequency stimulation would disturb the determination of the quantal size by the variance-mean analysis with my stimulation protocol. Therefore, I performed the same series of experiments in the presence of 100 μ M cyclothiazide (CTZ), which is known to slow the desensitization of AMPA-type glutamate receptors. As shown in Fig. 3-6A, EPSCs recorded in the presence of 100 μ M CTZ showed prolonged decay times, and the EPSC decay was not completed when the subsequent stimulus was applied at 200 Hz. The amplitudes of the EPSCs during the trains were therefore calculated from differences between the peaks and the current remaining from the previous EPSCs (Fig. 3-6, right). This analysis revealed that the quantal size estimated from the variance-mean analysis in the presence of CTZ did not significantly differ from those without the drug (Fig. 3-6C, D), indicating that the receptor desensitization during the high frequency stimulation did not hamper the determination of the quantal size under this protocol.

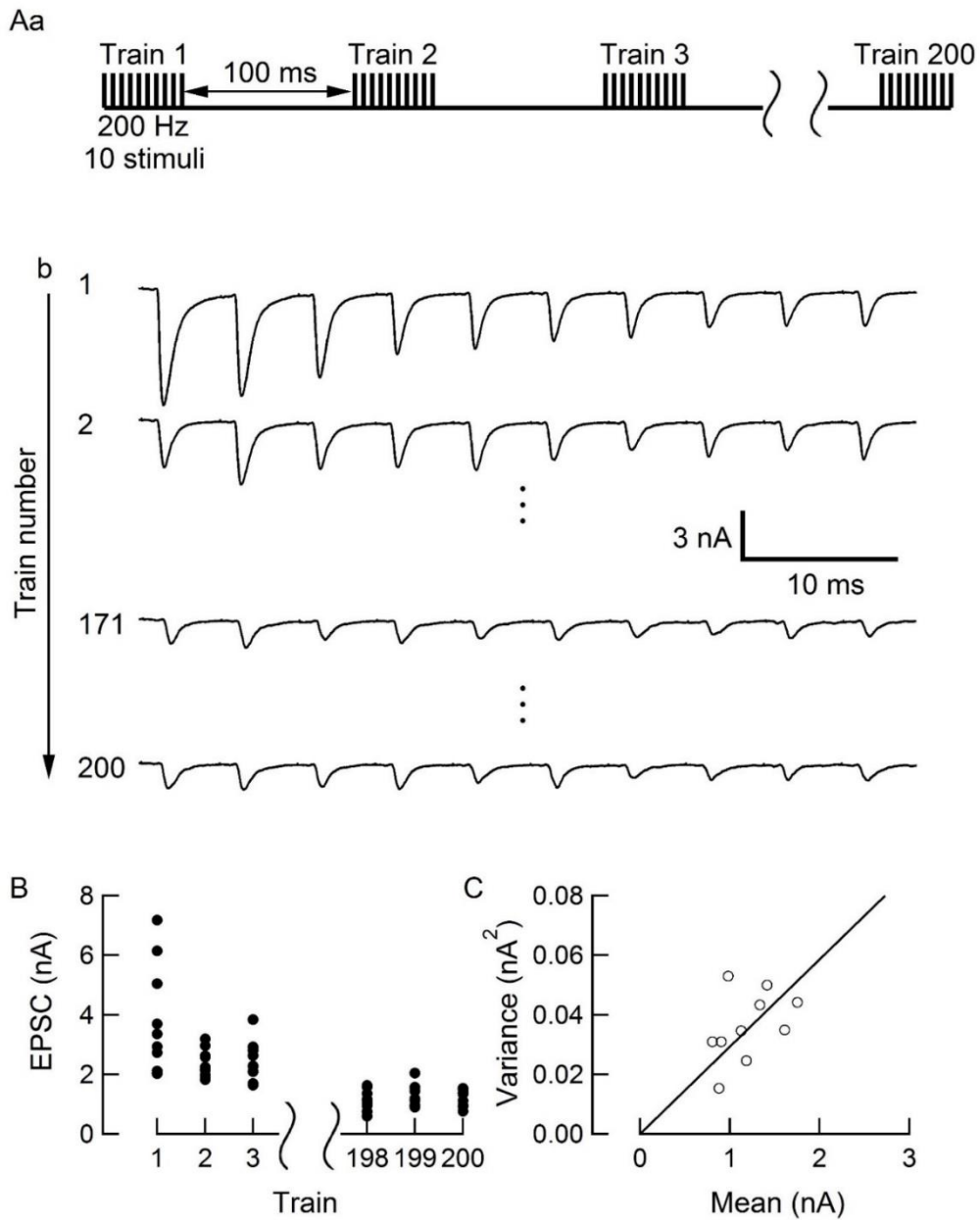


Figure 3-5. Nonstationary variance-mean analysis in the presence of glutamate.

A. a. A experimental protocol. b. Sample traces of EPSCs evoked by a series of high frequency stimuli. B. The magnitude of EPSCs evoked by the repeated high frequency stimulation. The first EPSC amplitude of the train 1 is 7.1 nA and tenth EPSC amplitude of the train 1 is 2.0 nA. The first EPSC amplitude of the train 200 is 1.5 nA and tenth EPSC amplitude of the train 200 is 0.9 nA. C. The resulting EPSC variance-mean plot in train 171-200, fitted by linear regression with a slope of 29.3 pA. Data in A-C are from the same cell.

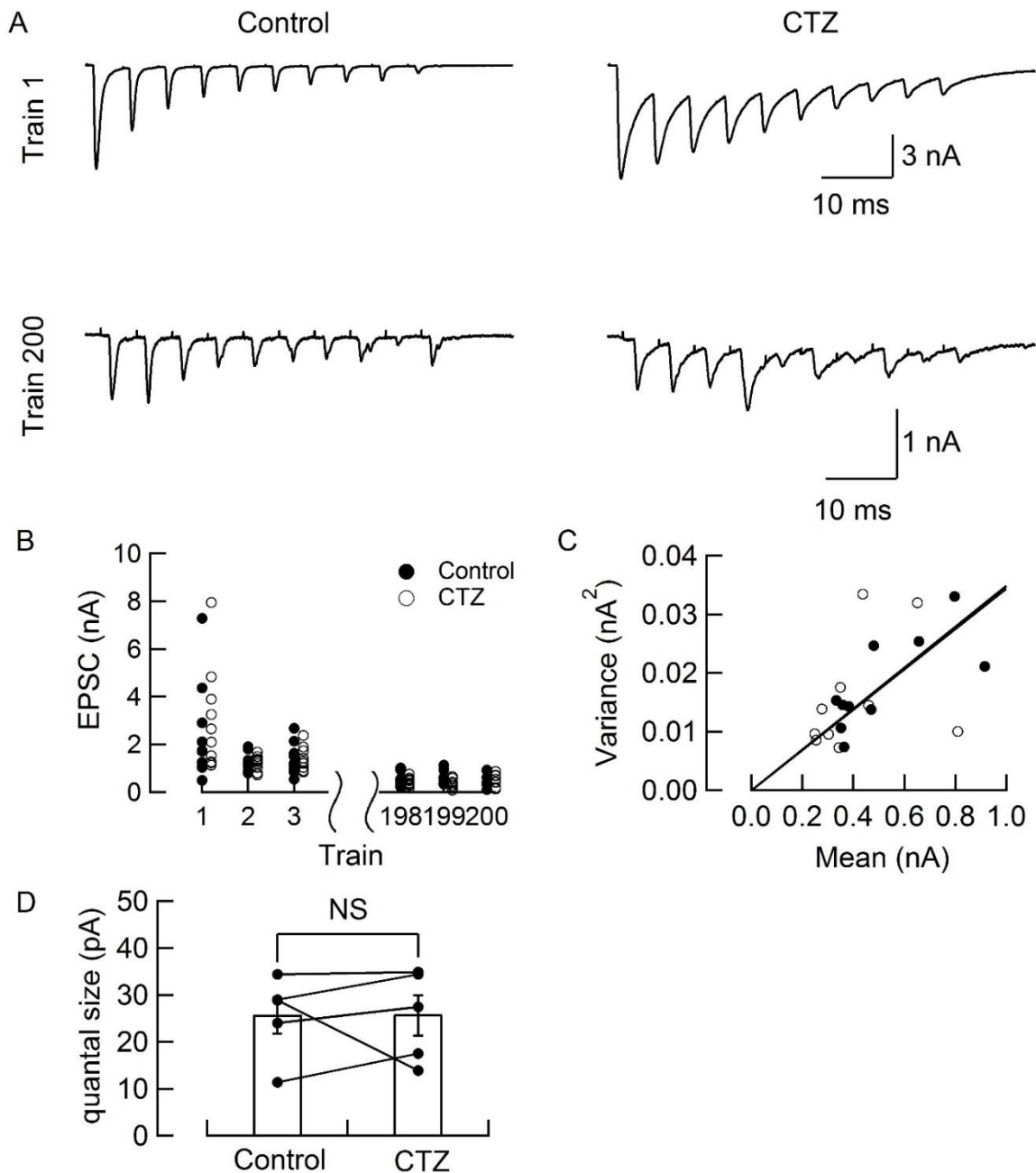


Figure 3-6. Nonstationary analysis in the presence of CTZ.

A. Sample traces of EPSCs before (left) and after (right) applying 100 μm CTZ. Upper trace is the EPSCs of train1, and lower trace is that of train 200. EPSCs recorded at one protocol was first measured under control, followed by measurements with CTZ. **B.** The magnitude of EPSC before (filled circle) and after (open circle) applying CTZ. The first EPSC amplitude of the train 1 is 7.2 (control) and 7.9 (CTZ) nA, and tenth EPSC amplitude of the train1 is 0.5 and 1.1nA. The first EPSC of the train 200 is 0.9 and 0.7 nA, and the tenth EPSC of the train200 is 0.4 and 0.19 nA. **C.** The resulting EPSC variance-mean plot in train 171-200, fitted by linear regression with a slope of 34.3 (control) and 34.8 (CTZ) pA. Data in A-C are from the same cell. **D.** The mean quantal size estimated by the nonstationary analysis. Each data derived from five experiments. No significant difference (N.S., $P>0.1$) was observed.

3.6. The variance-mean analysis reliably reports changes of quantal size during repetitive stimulation.

To further validate whether the variance-mean analysis can indeed detect changes of quantal size during the repetitive stimulation, I tested the effect of partial blockade of the postsynaptic AMPA receptors by applying CNQX at incremental concentrations (0.2-1.5 μ M, Fig. 3-7). Fig 3-7 shows the results from a representative cell where AMPA receptors were partially blocked by 1.5 μ M CNQX. The mean EPSC amplitude decreased from 8.0 ± 0.2 nA (0 μ M CNQX) to 2.1 ± 0.5 nA (1.5 μ M CNQX). Furthermore, the quantal size estimated by the variance-mean analysis also decreased from 28 ± 2.2 pA (0 μ M CNQX) to 6.3 ± 0.5 pA (1.5 μ M CNQX) (n=5 cells). All the results from various concentrations of CNQX were summarized in Fig. 3-7, clearly indicating that the quantal size decreased as CNQX concentration increased. When both EPSCs amplitudes and quantal sizes calculated from the analysis were normalized to those of control condition (0 μ M CNQX) and plotted as a function of CNQX concentrations, EPSCs and quantal sizes decreased to the same extent (Fig 3-7), indicating that this analysis faithfully reports the reduction of average quantal size constituting the evoked EPSCs.

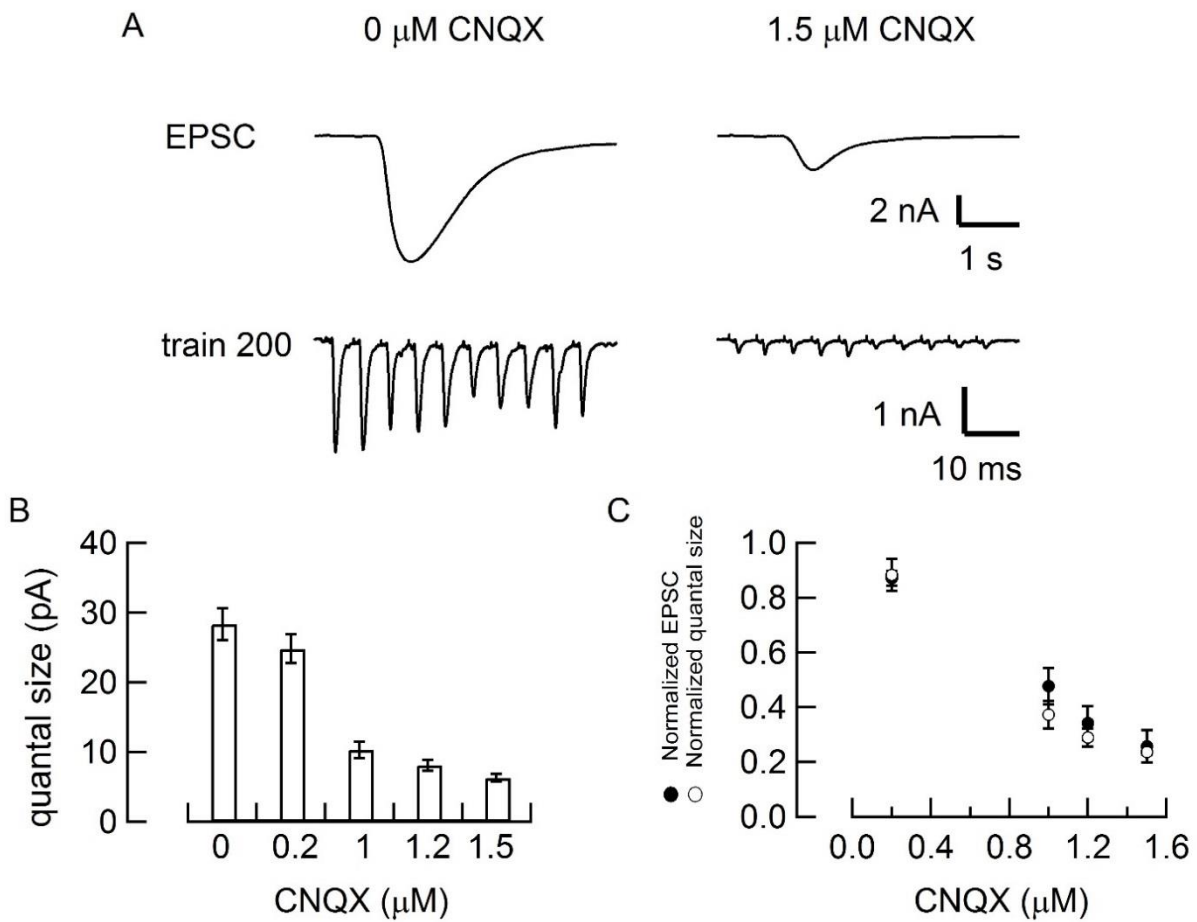


Figure 3-7. Pharmacological reduction of quantal size by applying CNQX.

A. Sample traces of EPSCs under the conditions of applying normal aCSF (left) and 1.5 μ M CNQX (right). upper trace is the first EPSC of train1, and lower traces are EPSCs of train 200. EPSCs recorded at one protocol was first measured under control, followed by measurements with incrementally CNQX concentrations. B. The mean quantal size estimated by the nonstationary analysis. Each data derived from five experiments. The mean quantal size is 28 ± 2.2 , 25 ± 2.0 , 10 ± 1.2 , 8.0 ± 0.7 , and 6.3 ± 0.5 pA (0, 0.2, 1, 1.2, and 1.5 μ M CNQX). C. EPSC amplitude (filled circle) and quantal size estimated by the nonstationary analysis (open circle) normalized to the control (0 μ M CNQX).

3.7. Quantal size during repetitive stimulation markedly decreased in the absence of cytosolic glutamate.

Having confirmed the reliability of the protocol to measure the quantal size during repetitive stimulation using the variance-mean analysis, I next performed similar experiments under the whole-cell dialysis of presynaptic cytosol with a glutamate free solution (Fig 3-8). Although I attempted to monitor time-dependent changes in evoked EPSC amplitudes and the corresponding quantal sizes systematically up to 30 min after the rapture of the presynaptic membrane, it turned out to be difficult to achieve such analysis, since EPSCs evoked by a train of action potentials after 30 min often became too small to be subjected to the variance-mean analysis. I, therefore, decided to apply a train of action potentials at 20 min after the establishment of whole-cell recordings, and the EPSCs during the last 30 trains of the high frequency stimulation were analyzed. Figure 3-8A depicts a recording paradigm and representative traces of evoked EPSCs. The initial evoked EPSC ($t = 0$) was recorded upon a single action potential and used to normalize subsequent EPSCs. Before giving the high frequency stimulation, mEPSCs were recorded for comparison for 30 s at 0 and 20 min.

As expected, the evoked EPSC amplitudes exhibited rundown at 20 min (~40 % of the initial EPSC amplitudes), whereas the reduction of mEPSC amplitudes was not comparable (~60 % of the initial mEPSC amplitudes) (Fig. 3-8B, left and center). On the other hand, the average quantal size estimated by the variance-mean analysis was not decreased by glutamate washout (Fig. 3-8B, right). However, it is possible that the extent of glutamate washout varied among cells, which caused variability of quantal sizes and has masked the effect of glutamate washout on the quantal size in the current

unpaired analyses. Unfortunately, paired analyses (before and after glutamate dialysis in the same cell) is not possible even with my short protocol. Therefore, I attempted to apply in-depth analyses of the data to determine whether substantial glutamate leak occurs or not. I first plotted the estimated quantal size against the amplitude of evoked EPSC at 20 min after the whole-cell recordings (Fig. II-4C). Although quantal sizes under control condition (3 mM glutamate) were constant irrespective of the size of EPSC amplitudes, quantal sizes after glutamate washout showed a positive correlation with the EPSC amplitudes (Fig. 3-8C). This implies that the variation of EPSC amplitudes under control conditions might result from differences in $N \cdot p$ in different cells, whereas that after glutamate washout might result from a difference in the mean quantal size (q). It is consistent with the hypothesis that empty vesicles accumulated, though we cannot completely exclude the possibility of slow glutamate leak.

In contrast, when mEPSC amplitudes after glutamate washout were plotted against normalized EPSC amplitudes, there was no clear correlation among them (Fig 3-8D). However, *undetectable* mEPSC events, which could be estimated from the reduction of mEPSC frequencies in the presence of CNQX (Fig. 3-3D), may have resulted in an overestimation of the average mEPSC amplitude calculated based on the *detected* events. To take this factor into account, the recorded mEPSC amplitudes were converted to compensate mEPSC amplitudes by adding a fraction of undetectable miniature events where their amplitudes were assumed to be 0 pA (here I assume that most of them are empty vesicles from recycling without the cytosolic glutamate, see Appendix). This data conversion resulted in a steeper slope of the linear regression and smaller y-axis intercept, indicating

that the results from mEPSC measurements, in fact, implicated that the average quantal size was reduced during glutamate washout, and the overall results are consistent between variance-mean analysis and the analysis of mEPSCs, if undetected events were taken into account. However, the extent of reduction cannot precisely be estimated with the current method lacking the paired analysis but appears not to be significant, which is also consistent with the estimation from the mEPSC analyses.

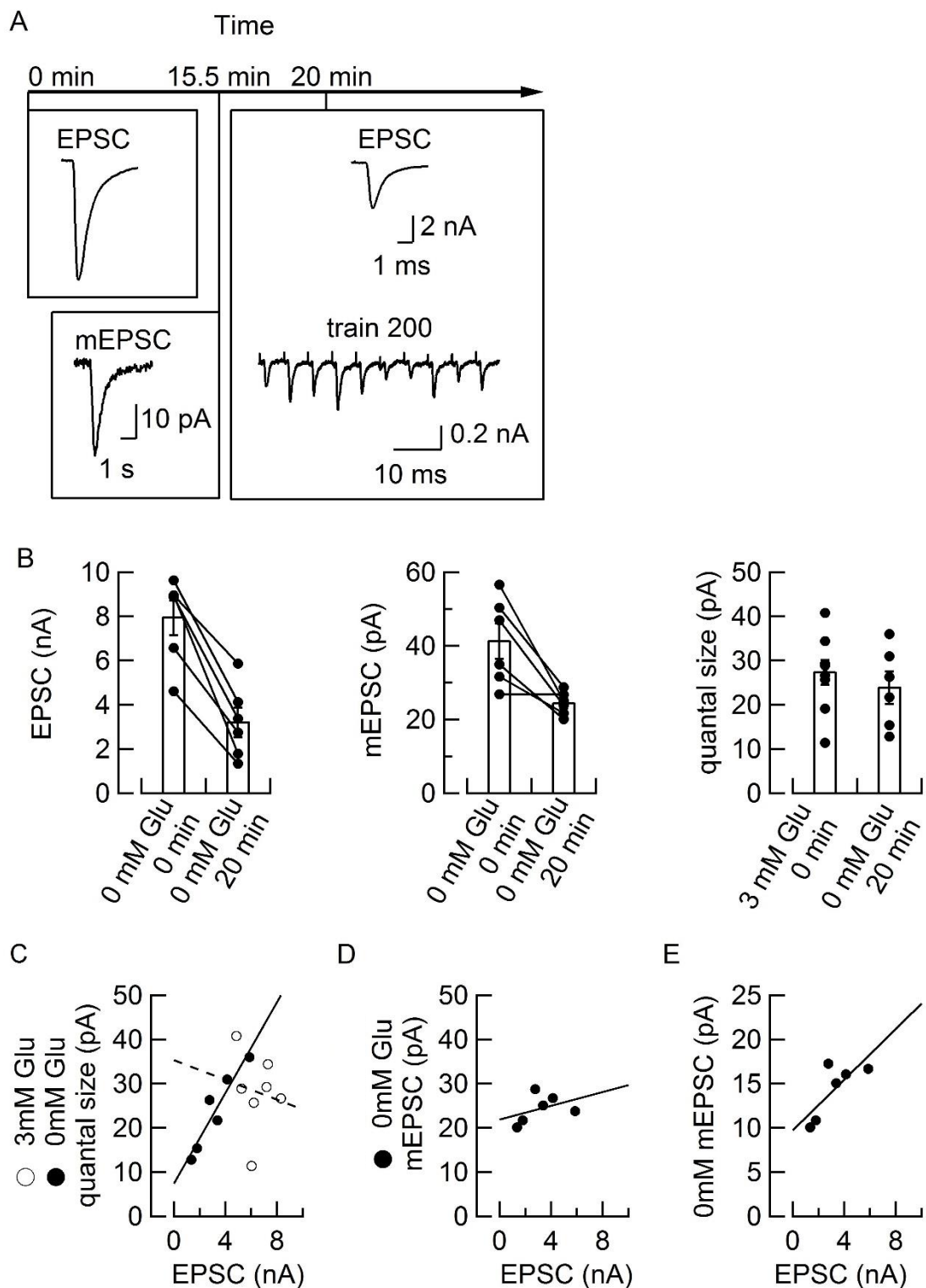


Fig. 3-8 mEPSC amplitude and quantal size estimated by nonstationary analysis after whole-cell washout of glutamate in the presynaptic terminal.

A. Sample trace of evoked EPSC just after whole-cell of pipettes. When glutamate washout for 20 min, we recorded mEPSCs for 30 sec, evoked EPSC, and a train of EPSCs for the nonstationary variance-mean analysis. B. EPSC (left) and mEPSC (middle) amplitude 0 and 20 min after glutamate washout. Right graph is the quantal size estimated by estimated by

nonstationary analysis. C. The relationship between quantal size under 3 mM glutamate (open circles) or 0 mM glutamate (filled circles) against the evoked EPSC amplitude. Each data point represents the data from individual cells. The line fits show the tendency in 0 mM (solid line) or 3 mM glutamate (dotted line). D. The relationship between mEPSC amplitudes and the evoked EPSC amplitudes in 0 mM glutamate. E. The same as D, but undetected events were taken into account by assuming that they were 0 pA. Frequency of undetected events was estimated from CNQX experiments shown in Fig 3.3.

4. Discussion

At the calyx of Held presynaptic terminal, the whole-cell dialysis of cytosolic glutamate slightly reduced the spontaneous mEPSC amplitude, and strongly reduced the evoked EPSC amplitude in this study. The relatively small rundown of mEPSCs after Baf treatment has previously been attributed to an artifact due to limited detectability of mEPSCs (Zhou et al, 2000). I have excluded this possibility, because the average amplitude of mEPSC events during glutamate washout was much larger than that under CNQX treatment at a given frequency, which reflects detectability of mEPSC amplitudes (assuming that CNQX or glutamate washout does not change N or Pr). The number of vesicles undergoing exocytosis during 30 min period of glutamate washout was estimated to be 513 ± 195 ($n=5$ pairs) from EPSCs evoked every 10 min, and $24,700 \pm 6,700$ ($n=5$ pairs) from spontaneous mEPSC that occurred 15 ± 4.2 Hz ($n=5$ pairs) on average. Since the total number of vesicles is estimated as 200,000 in a calyx of Held terminal (De Lange et al. 2003), ~13% of total vesicles underwent spontaneous exocytosis and recycled without being refilled with glutamate. Given that a fraction of total vesicles undergoes recycling in physiological condition (Rizzoli & Betz, 2005; but see Xue et al. 2013), relatively stronger rundown of evoked EPSCs after blocking glutamate uptake can be explained by the accumulation of empty vesicles following spontaneous and evoked release through vesicle recycling without cytosolic glutamate. It is controversial whether the recycling pool of vesicles undergoing spontaneous exocytosis is distinct from that used for evoked exocytosis (Chung et al. 2010; Wilhelm et al. 2010). At the calyx of Held, marked reductions of mEPSC

frequency and evoked EPSC amplitude after blocking glutamate uptake suggest that their recycling pools are overlapped, at least to some extent.

At hippocampal synapses in culture, Zhou et al. (2000) reported that Baf treatment (1 μ M, at 37 °C for 1 h) reduces mEPSC amplitude to ~60 % of controls, with little further reduction after longer treatment, whereas Ikeda & Bekkers (2009) saw no significant reduction in mEPSC amplitude ~10 min after local Baf application (5 μ M, 100 s, at RT). At the calyx of Held, bath-applied Baf (5 μ M, 100 s) decreased mEPSC amplitude to 70 % of controls, and glutamate washout decreased it to 80 % in 30 min. The real reduction of mEPSCs should be much more, if we take undetected events into account. Because the reduced amplitude of mEPSC were still larger than those expected from the detection limit probed by CNQX experiments, it is likely that some synaptic vesicles maintain glutamate for 30 min in the absence of cytosolic glutamate until they undergo exocytosis, favoring for the possibility of little glutamate leakage. However, we cannot entirely exclude the possibility that the reduced mEPSC amplitudes after glutamate washout or Baf application indeed reflected the magnitude of glutamate leakage out of vesicles at least to some extent. This leakage is normally compensated by uptake of glutamate from presynaptic cytosol using proton gradient produced by vacuolar ATPase, as there was no change in the mEPSC amplitude at least for 30 min in the presence of 3 mM glutamate in presynaptic pipettes (Fig. 3-1, see also Ishikawa et al. 2002).

Based on the assumption that glutamate does not leak out of vesicles, Ikeda & Bekkers (2009) calculated the number of recycling vesicles by dividing total EPSC charge over 30-40 min by a single mEPSC charge. Because of its minor influence on synaptic efficacy, glutamate leakage may not much

affect such calculations. However, since the spontaneous mEPSC frequency can affect the magnitude of EPSC rundown after blocking glutamate uptake, estimation of the functional vesicle pool size should take this factor into account, unless vesicle recycling after evoked and spontaneous release are totally independent. Furthermore, although Ikeda & Bekkers concluded that mild stimulation could mobilize all vesicle pools including the reserve pool, it is uncertain at the calyx of Held where it is still under debate regarding an exact fraction of recycling vesicles within the total vesicles in the terminals (Rizzoli & Betz, 2005; but see Xue et al. 2013). At present, therefore, we cannot estimate the size of recycling vesicle pool using such calculation at the calyx of Held.

In isolated preparations, glutamate leaks out of vesicles when vesicular proton gradient is dissipated (Carlson & Ueda, 1990; Maycox et al. 1990). GABA, but neither glutamate nor glycine, can permeate phospholipid liposomes without vesicular protein (Hell et al, 1991; Schenck et al, 2009), whereas glutamate leakage is reportedly caused by the H⁺/glutamate antiport through vesicular glutamate transporters (VGLUTs; Mackenzie et al, 2008). The calyces of Held in rodents express both VGLUT1 and VGLUT2 (Billups, 2005; Blaesse et al, 2005). Thus, it remains to be seen whether the magnitude of glutamate leakage is different between vesicles expressing different VGLUT subtypes, meaning that some synaptic vesicles leak glutamate whereas others not.

Nevertheless, the present study demonstrates that the leakage of glutamate from synaptic vesicles seems to be minimized in the *in vivo* condition, compared to *in vitro* conditions (Carlson & Ueda, 1990; Maycox et al. 1990), although a small amount of leakage cannot be excluded. Relatively little leakage would economize consumption of energy to fill vesicles with glutamate and reduce variability

of glutamate concentration because balance between filling and glutamate may vary the concentration at rest, increasing fluctuation of EPSCs. A large number of recycling vesicles at the calyx of Held minimize a fraction of empty vesicles because not all vesicles would be used up during repetitive activity. Overall, the calyx of Held is highly optimized for reliable synaptic transmission, which is required for high-frequency signaling in the auditory pathways (von Gersdorff and Borst, 2002). It remains to be studied if the present observations are applicable to mammalian CNS synapses in general.

Appendix. Technical concerns on the non-stationary fluctuation analysis

Since I used EPSCs during sustained phase for the fluctuation analysis where release probabilities were extremely low, it was not possible to fit the variance-mean relationship with a parabola. Thus, an initial slope of a linear regression was calculated from the plot to estimate quantal size (q) (Meyer et al., 2001). Compared to the stationary fluctuation analysis (Silver et al., 1998), other quantal parameters such as N and P_r could not be deduced with this method. One way to circumvent this problem is to increase the release probability by using high extracellular $[Ca^{2+}]$ during recordings. However, AMPA receptor saturation and desensitization would severely affect the estimate of quantal size (Meyer et al., 2001; Schuess et al., 2002). Therefore, if quantal size is the only parameter of interest, the current protocol will be useful to measure it feasibly with quick experiments.

With strong repetitive stimulation adopted here for the fluctuation analysis, there are several possible drawbacks which would cause an underestimation of quantal size. Namely, AMPA receptor desensitization during intense stimulation may affect the estimation (Koike-Tani et al., 2008). It was demonstrated that desensitization occurs at immature state (P8-10), which disappears at more mature state (P16-18) after hearing onset (P10-12; Futai et al., 2001). Although I performed experiments after hearing onset (P13-16), I experimentally validated the effect of CTZ on the estimated quantal size and found no significant effect. Therefore, the underestimation of quantal size attributed to receptor desensitization is negligible.

Additionally, saturation of available AMPA receptors at the postsynaptic sites may also result in the underestimation. This possibility can be experimentally ruled out by using kynurenic acid, a low affinity competitive AMPA receptor antagonist with a fast unblocking time constant. However, amplitudes of EPSCs detected at the later phase of the train stimulation with kynurenic acid will be hardly detected in the absence of cytosolic glutamate. Considering extremely low release probability at the sustained phases, glutamate concentrations at the synaptic cleft should not saturate the postsynaptic receptors even in the presence of 3 mM glutamate in the pipette. Collectively, the reduction of quantal size estimated here during glutamate washout is likely resulted from reduction of glutamate in synaptic vesicles.

Acknowledgments

First and foremost, I would like to thank Prof. Dr. Tomoyuki Takahashi not only for his invaluable support and guidance throughout this PhD project but also because he shares his enthusiasm and love for science with me. He selflessly donated a great amount of effort on training me the basic skills for my career. During my first few years working with him, he spent a lot of time with me in investigating the experiment results. I benefit a lot of this training in my future career. To improve my English, he carefully commented on all my paper draft. I was quite fortunate to have Prof. Takahashi as my advisor. Many thanks go to Dr. Tetsuya Hori for patiently helping me face the challenges and sustain my motivation. I would like to thank him also for his constant support, scientific inputs and technical assistance throughout my PhD from the first steps of developing the assay to writing the manuscript and the thesis. I also want to thank my collaborators in OIST, Kohgaku Eguchi. Our work requires his technique of capacitance measurement. Without his expertise and help, I could not have completed my thesis. He is always passionate and responsive.

I would like to express my gratitude to Prof. Dr. Shigeo Takamori. After moving Takahashi laboratory to OIST, he always takes notice of me, and advises for my PhD project and carrer. His enthusiasm for research and relentless pursuit of excellence were a great inspiration for me. I acknowledge Dr. Manami Yamashita for her close friendship, scientific discussions. During spending time, I learned a lot from her. I would like to thank all the past and present members of Takahashi laboratory for providing a nice and friendly working atmosphere especially Dr. Nakamura, Dr. Miki and the secretary, Mrs. Yui. I could not have done this without the love and support of my family. They are

part of what keeps me going through the challenges in graduate school. To my mother, Sakiko Ohyama, thank you for all love and support you provided to me. Thank you to my loving husband, Kyosuke, for the constant support and encouragement.

Bibliography

- Bartoletti TM & Thoreson WB. (2011). Quantal amplitude at the cone ribbon synapse can be adjusted by changes in cytosolic glutamate. *Molecular vision* 17, 920-931.
- Bellocchio EE, Reimer RJ, Fremeau RT, Jr. & Edwards RH. (2000). Uptake of glutamate into synaptic vesicles by an inorganic phosphate transporter. *Science (New York, NY)* 289, 957-960.
- Billups B. (2005). Colocalization of vesicular glutamate transporters in the rat superior olivary complex. *Neuroscience letters* 382, 66-70.
- Birks R, Huxley HE & Katz B. (1960). The fine structure of the neuromuscular junction of the frog. *The Journal of physiology* 150, 134-144.
- Blaesse P, Ehrhardt S, Friauf E & Nothwang HG. (2005). Developmental pattern of three vesicular glutamate transporters in the rat superior olivary complex. *Cell and tissue research* 320, 33-50.
- Burger PM, Mehl E, Cameron PL, Maycox PR, Baumert M, Lottspeich F, De Camilli P & Jahn R. (1989). Synaptic vesicles immunisolated from rat cerebral cortex contain high levels of glutamate. *Neuron* 3, 715-720.
- Carlson MD & Ueda T. (1990). Accumulated glutamate levels in the synaptic vesicle are not maintained in the absence of active transport. *Neuroscience letters* 110, 325-330.
- Chapman ER. (2008). How does synaptotagmin trigger neurotransmitter release? *Annual review of biochemistry* 77, 615-641.
- Chung C, Barylko B, Leitz J, Liu X & Kavalali ET. (2010). Acute dynamin inhibition dissects

synaptic vesicle recycling pathways that drive spontaneous and evoked neurotransmission.

The Journal of neuroscience : the official journal of the Society for Neuroscience 30, 1363-1376.

Clements JD & Silver RA. (2000). Unveiling synaptic plasticity: a new graphical and analytical approach. *Trends in neurosciences* 23, 105-113.

Daniels RW, Collins CA, Chen K, Gelfand MV, Featherstone DE & DiAntonio A. (2006). A single vesicular glutamate transporter is sufficient to fill a synaptic vesicle. *Neuron* 49, 11-16.

Daniels RW, Collins CA, Gelfand MV, Dant J, Brooks ES, Krantz DE & DiAntonio A. (2004). Increased expression of the *Drosophila* vesicular glutamate transporter leads to excess glutamate release and a compensatory decrease in quantal content. *The Journal of neuroscience : the official journal of the Society for Neuroscience* 24, 10466-10474.

de Lange RP, de Roos AD & Borst JG. (2003). Two modes of vesicle recycling in the rat calyx of Held. *The Journal of neuroscience : the official journal of the Society for Neuroscience* 23, 10164-10173.

Del Castillo J & Katz B. (1954). Quantal components of the end-plate potential. *The Journal of physiology* 124, 560-573.

Edwards RH. (2007). The neurotransmitter cycle and quantal size. *Neuron* 55, 835-858.

Eguchi K, Nakanishi S, Takagi H, Taoufiq Z & Takahashi T. (2012). Maturation of a PKG-dependent retrograde mechanism for exoendocytic coupling of synaptic vesicles. *Neuron* 74, 517-529.

Fatt P & Katz B. (1952). Spontaneous subthreshold activity at motor nerve endings. *The Journal of*

physiology 117, 109-128.

Fenster SD, Chung WJ, Zhai R, Cases-Langhoff C, Voss B, Garner AM, Kaempf U, Kindler S,

Gundelfinger ED & Garner CC. (2000). Piccolo, a presynaptic zinc finger protein structurally related to bassoon. *Neuron* 25, 203-214.

Fremeau RT, Jr., Burman J, Qureshi T, Tran CH, Proctor J, Johnson J, Zhang H, Sulzer D, Copenhagen

DR, Storm-Mathisen J, Reimer RJ, Chaudhry FA & Edwards RH. (2002). The identification of vesicular glutamate transporter 3 suggests novel modes of signaling by glutamate.

Proceedings of the National Academy of Sciences of the United States of America 99, 14488-14493.

Fremeau RT, Jr., Kam K, Qureshi T, Johnson J, Copenhagen DR, Storm-Mathisen J, Chaudhry FA,

Nicoll RA & Edwards RH. (2004). Vesicular glutamate transporters 1 and 2 target to functionally distinct synaptic release sites. *Science (New York, NY)* 304, 1815-1819.

Goh GY, Huang H, Ullman J, Borre L, Hnasko TS, Trussell LO & Edwards RH. (2011). Presynaptic

regulation of quantal size: K⁺/H⁺ exchange stimulates vesicular glutamate transport. *Nature neuroscience* 14, 1285-1292.

Hamill OP, Marty A, Neher E, Sakmann B & Sigworth FJ. (1981). Improved patch-clamp techniques

for high-resolution current recording from cells and cell-free membrane patches. *Pflügers Archiv : European journal of physiology* 391, 85-100.

Harata N, Ryan TA, Smith SJ, Buchanan J & Tsien RW. (2001). Visualizing recycling synaptic

vesicles in hippocampal neurons by FM 1-43 photoconversion. *Proceedings of the National*

Academy of Sciences of the United States of America 98, 12748-12753.

Hata Y, Slaughter CA & Sudhof TC. (1993). Synaptic vesicle fusion complex contains unc-18 homologue bound to syntaxin. *Nature* 366, 347-351.

He L & Wu LG. (2007). The debate on the kiss-and-run fusion at synapses. *Trends in neurosciences* 30, 447-455.

He L, Wu XS, Mohan R & Wu LG. (2006). Two modes of fusion pore opening revealed by cell-attached recordings at a synapse. *Nature* 444, 102-105.

Hell JW, Edelmann L, Hartinger J & Jahn R. (1991). Functional reconstitution of the gamma-aminobutyric acid transporter from synaptic vesicles using artificial ion gradients. *Biochemistry* 30, 11795-11800.

Herman MA, Ackermann F, Trimbuch T & Rosenmund C. (2014). Vesicular glutamate transporter expression level affects synaptic vesicle release probability at hippocampal synapses in culture. *The Journal of neuroscience : the official journal of the Society for Neuroscience* 34, 11781-11791.

Heuser JE & Reese TS. (1973). Evidence for recycling of synaptic vesicle membrane during transmitter release at the frog neuromuscular junction. *The Journal of cell biology* 57, 315-344.

Hnasko TS, Chuhma N, Zhang H, Goh GY, Sulzer D, Palmiter RD, Rayport S & Edwards RH. (2010). Vesicular glutamate transport promotes dopamine storage and glutamate corelease in vivo. *Neuron* 65, 643-656.

- Hodgkin AL & Huxley AF. (1952). Currents carried by sodium and potassium ions through the membrane of the giant axon of Loligo. *The Journal of physiology* 116, 449-472.
- Hori T & Takahashi T. (2012). Kinetics of synaptic vesicle refilling with neurotransmitter glutamate. *Neuron* 76, 511-517.
- Hori T, Takai Y & Takahashi T. (1999). Presynaptic mechanism for phorbol ester-induced synaptic potentiation. *The Journal of neuroscience : the official journal of the Society for Neuroscience* 19, 7262-7267.
- Huang H & Trussell LO. (2014). Presynaptic HCN channels regulate vesicular glutamate transport. *Neuron* 84, 340-346.
- Ikeda K & Bekkers JM. (2009). Counting the number of releasable synaptic vesicles in a presynaptic terminal. *Proceedings of the National Academy of Sciences of the United States of America* 106, 2945-2950.
- Ishikawa T, Sahara Y & Takahashi T. (2002). A single packet of transmitter does not saturate postsynaptic glutamate receptors. *Neuron* 34, 613-621.
- Jahn R & Fasshauer D. (2012). Molecular machines governing exocytosis of synaptic vesicles. *Nature* 490, 201-207.
- Katz B & Miledi R. (1969). Spontaneous and evoked activity of motor nerve endings in calcium Ringer. *The Journal of physiology* 203, 689-706.
- Kim SH & Ryan TA. (2010). CDK5 serves as a major control point in neurotransmitter release. *Neuron* 67, 797-809.

- Koike-Tani M, Kanda T, Saitoh N, Yamashita T & Takahashi T. (2008). Involvement of AMPA receptor desensitization in short-term synaptic depression at the calyx of Held in developing rats. *The Journal of physiology* 586, 2263-2275.
- Lenn NJ & Reese TS. (1966). The fine structure of nerve endings in the nucleus of the trapezoid body and the ventral cochlear nucleus. *The American journal of anatomy* 118, 375-389.
- Lindau M & Neher E. (1988). Patch-clamp techniques for time-resolved capacitance measurements in single cells. *Pflugers Archiv : European journal of physiology* 411, 137-146.
- Mackenzie B, Illing AC, Morris ME, Varoqui H & Erickson JD. (2008). Analysis of a vesicular glutamate transporter (VGLUT2) supports a cell-leakage mode in addition to vesicular packaging. *Neurochemical research* 33, 238-247.
- Marshansky V, Rubinstein JL & Gruber G. (2014). Eukaryotic V-ATPase: novel structural findings and functional insights. *Biochimica et biophysica acta* 1837, 857-879.
- Masson J, Darmon M, Conjard A, Chuhma N, Ropert N, Thoby-Brisson M, Foutz AS, Parrot S, Miller GM, Jorisch R, Polan J, Hamon M, Hen R & Rayport S. (2006). Mice lacking brain/kidney phosphate-activated glutaminase have impaired glutamatergic synaptic transmission, altered breathing, disorganized goal-directed behavior and die shortly after birth. *The Journal of neuroscience : the official journal of the Society for Neuroscience* 26, 4660-4671.
- Maycox PR, Deckwerth T, Hell JW & Jahn R. (1988). Glutamate uptake by brain synaptic vesicles. Energy dependence of transport and functional reconstitution in proteoliposomes. *The Journal of biological chemistry* 263, 15423-15428.

- Maycox PR, Deckwerth T & Jahn R. (1990). Bacteriorhodopsin drives the glutamate transporter of synaptic vesicles after co-reconstitution. *The EMBO journal* 9, 1465-1469.
- Meinrenken CJ, Borst JG & Sakmann B. (2002). Calcium secretion coupling at calyx of Held governed by nonuniform channel-vesicle topography. *The Journal of neuroscience : the official journal of the Society for Neuroscience* 22, 1648-1667.
- Meyer AC, Neher E & Schneggenburger R. (2001). Estimation of quantal size and number of functional active zones at the calyx of Held synapse by nonstationary EPSC variance analysis. *The Journal of neuroscience : the official journal of the Society for Neuroscience* 21, 7889-7900.
- Moechars D, Weston MC, Leo S, Callaerts-Vegh Z, Goris I, Daneels G, Buist A, Cik M, van der Spek P, Kass S, Meert T, D'Hooge R, Rosenmund C & Hampson RM. (2006). Vesicular glutamate transporter VGLUT2 expression levels control quantal size and neuropathic pain. *The Journal of neuroscience : the official journal of the Society for Neuroscience* 26, 12055-12066.
- Naito S & Ueda T. (1985). Characterization of glutamate uptake into synaptic vesicles. *Journal of neurochemistry* 44, 99-109.
- Omote H & Moriyama Y. (2013). Vesicular neurotransmitter transporters: an approach for studying transporters with purified proteins. *Physiology (Bethesda, Md)* 28, 39-50.
- Reger JF. (1958). The fine structure of neuromuscular synapses of gastrocnemii from mouse and frog. *The Anatomical record* 130, 7-23.
- Rizo J, Chen X & Arac D. (2006). Unraveling the mechanisms of synaptotagmin and SNARE

- function in neurotransmitter release. *Trends in cell biology* 16, 339-350.
- Rizzoli SO & Betz WJ. (2005). Synaptic vesicle pools. *Nature reviews Neuroscience* 6, 57-69.
- Rosenmund C & Stevens CF. (1996). Definition of the readily releasable pool of vesicles at hippocampal synapses. *Neuron* 16, 1197-1207.
- Sahara Y & Takahashi T. (2001). Quantal components of the excitatory postsynaptic currents at a rat central auditory synapse. *The Journal of physiology* 536, 189-197.
- Sakaba T & Neher E. (2001). Calmodulin mediates rapid recruitment of fast-releasing synaptic vesicles at a calyx-type synapse. *Neuron* 32, 1119-1131.
- Schenck S, Wojcik SM, Brose N & Takamori S. (2009). A chloride conductance in VGLUT1 underlies maximal glutamate loading into synaptic vesicles. *Nature neuroscience* 12, 156-162.
- Schikorski T & Stevens CF. (1997). Quantitative ultrastructural analysis of hippocampal excitatory synapses. *The Journal of neuroscience : the official journal of the Society for Neuroscience* 17, 5858-5867.
- Seal RP, Akil O, Yi E, Weber CM, Grant L, Yoo J, Clause A, Kandler K, Noebels JL, Glowatzki E, Lustig LR & Edwards RH. (2008). Sensorineural deafness and seizures in mice lacking vesicular glutamate transporter 3. *Neuron* 57, 263-275.
- Silver RA, Momiyama A & Cull-Candy SG. (1998). Locus of frequency-dependent depression identified with multiple-probability fluctuation analysis at rat climbing fibre-Purkinje cell synapses. *The Journal of physiology* 510 (Pt 3), 881-902.
- Sudhof TC & Rizo J. (2011). Synaptic vesicle exocytosis. *Cold Spring Harbor perspectives in biology*

3.

Sun JY, Wu XS & Wu LG. (2002). Single and multiple vesicle fusion induce different rates of endocytosis at a central synapse. *Nature* 417, 555-559.

Takago H, Nakamura Y & Takahashi T. (2005). G protein-dependent presynaptic inhibition mediated by AMPA receptors at the calyx of Held. *Proceedings of the National Academy of Sciences of the United States of America* 102, 7368-7373.

Takahashi T, Forsythe ID, Tsujimoto T, Barnes-Davies M & Onodera K. (1996). Presynaptic calcium current modulation by a metabotropic glutamate receptor. *Science (New York, NY)* 274, 594-597.

Takahashi T, Hori T, Kajikawa Y & Tsujimoto T. (2000). The role of GTP-binding protein activity in fast central synaptic transmission. *Science (New York, NY)* 289, 460-463.

Takamori S, Rhee JS, Rosenmund C & Jahn R. (2000). Identification of a vesicular glutamate transporter that defines a glutamatergic phenotype in neurons. *Nature* 407, 189-194.

tom Dieck S, Sanmarti-Vila L, Langnaese K, Richter K, Kindler S, Soyke A, Wex H, Smalla KH, Kampf U, Franzer JT, Stumm M, Garner CC & Gundelfinger ED. (1998). Bassoon, a novel zinc-finger CAG/glutamine-repeat protein selectively localized at the active zone of presynaptic nerve terminals. *The Journal of cell biology* 142, 499-509.

Verhage M, Maia AS, Plomp JJ, Brussaard AB, Heeroma JH, Vermeer H, Toonen RF, Hammer RE, van den Berg TK, Missler M, Geuze HJ & Sudhof TC. (2000). Synaptic assembly of the brain in the absence of neurotransmitter secretion. *Science (New York, NY)* 287, 864-869.

- von Gersdorff H & Borst JG. (2002). Short-term plasticity at the calyx of Held. *Nature reviews Neuroscience* 3, 53-64.
- Wallen-Mackenzie A, Gezelius H, Thoby-Brisson M, Nygard A, Enjin A, Fujiyama F, Fortin G & Kullander K. (2006). Vesicular glutamate transporter 2 is required for central respiratory rhythm generation but not for locomotor central pattern generation. *The Journal of neuroscience : the official journal of the Society for Neuroscience* 26, 12294-12307.
- Wang X, Kibschull M, Laue MM, Lichte B, Petrasch-Parwez E & Kilimann MW. (1999). Aczonin, a 550-kD putative scaffolding protein of presynaptic active zones, shares homology regions with Rim and Bassoon and binds profilin. *The Journal of cell biology* 147, 151-162.
- Wang Y, Okamoto M, Schmitz F, Hofmann K & Sudhof TC. (1997). Rim is a putative Rab3 effector in regulating synaptic-vesicle fusion. *Nature* 388, 593-598.
- Wang Y, Sugita S & Sudhof TC. (2000). The RIM/NIM family of neuronal C2 domain proteins. Interactions with Rab3 and a new class of Src homology 3 domain proteins. *The Journal of biological chemistry* 275, 20033-20044.
- Watanabe S, Rost BR, Camacho-Perez M, Davis MW, Sohl-Kielczynski B, Rosenmund C & Jorgensen EM. (2013). Ultrafast endocytosis at mouse hippocampal synapses. *Nature* 504, 242-247.
- Weber T, Zemelman BV, McNew JA, Westermann B, Gmachl M, Parlati F, Sollner TH & Rothman JE. (1998). SNAREpins: minimal machinery for membrane fusion. *Cell* 92, 759-772.
- Wilhelm BG, Groemer TW & Rizzoli SO. (2010). The same synaptic vesicles drive active and

spontaneous release. *Nature neuroscience* 13, 1454-1456.

Wilson NR, Kang J, Hueske EV, Leung T, Varoqui H, Murnick JG, Erickson JD & Liu G. (2005).

Presynaptic regulation of quantal size by the vesicular glutamate transporter VGLUT1. *The Journal of neuroscience : the official journal of the Society for Neuroscience* 25, 6221-6234.

Wojcik SM, Rhee JS, Herzog E, Sigler A, Jahn R, Takamori S, Brose N & Rosenmund C. (2004). An

essential role for vesicular glutamate transporter 1 (VGLUT1) in postnatal development and control of quantal size. *Proceedings of the National Academy of Sciences of the United States of America* 101, 7158-7163.

Wolosker H, de Souza DO & de Meis L. (1996). Regulation of glutamate transport into synaptic

vesicles by chloride and proton gradient. *The Journal of biological chemistry* 271, 11726-11731.

Wu XS, Xue L, Mohan R, Paradiso K, Gillis KD & Wu LG. (2007). The origin of quantal size

variation: vesicular glutamate concentration plays a significant role. *The Journal of neuroscience : the official journal of the Society for Neuroscience* 27, 3046-3056.

Xue L, Sheng J, Wu XS, Wu W, Luo F, Shin W, Chiang HC & Wu LG. (2013). Most vesicles in a

central nerve terminal participate in recycling. *The Journal of neuroscience : the official journal of the Society for Neuroscience* 33, 8820-8826.

Yamashita T, Eguchi K, Saitoh N, von Gersdorff H & Takahashi T. (2010). Developmental shift to a

mechanism of synaptic vesicle endocytosis requiring nanodomain Ca²⁺. *Nature neuroscience* 13, 838-844.

- Yamashita T, Hige T & Takahashi T. (2005). Vesicle endocytosis requires dynamin-dependent GTP hydrolysis at a fast CNS synapse. *Science (New York, NY)* 307, 124-127.
- Yamashita T, Ishikawa T & Takahashi T. (2003). Developmental increase in vesicular glutamate content does not cause saturation of AMPA receptors at the calyx of Held synapse. *The Journal of neuroscience : the official journal of the Society for Neuroscience* 23, 3633-3638.
- Yamashita T, Kanda T, Eguchi K & Takahashi T. (2009). Vesicular glutamate filling and AMPA receptor occupancy at the calyx of Held synapse of immature rats. *The Journal of physiology* 587, 2327-2339.
- Zhou Q, Lai Y, Bacaj T, Zhao M, Lyubimov AY, Uervirojnangkoorn M, Zeldin OB, Brewster AS, Sauter NK, Cohen AE, Soltis SM, Alonso-Mori R, Chollet M, Lemke HT, Pfuetzner RA, Choi UB, Weis WI, Diao J, Sudhof TC & Brunger AT. (2015). Architecture of the synaptotagmin-SNARE machinery for neuronal exocytosis. *Nature* 525, 62-67.
- Zhou Q, Petersen CC & Nicoll RA. (2000). Effects of reduced vesicular filling on synaptic transmission in rat hippocampal neurones. *The Journal of physiology* 525 Pt 1, 195-206.